PREPARATION AND CHARACTERIZATION OF HIGH TEMPERATURE SUPERCONDUCTING THIN FILMS

By

Steven K. Dew

B.A.Sc. University of British Columbia, 1987

A THESIS SUBMITTED IN PARTIAL FULFILLMENT OF

THE REQUIREMENTS FOR THE DEGREE OF

MASTER OF APPLIED SCIENCE

in

THE FACULTY OF GRADUATE STUDIES

ENGINEERING PHYSICS

We accept this thesis as conforming

to the required standard

THE UNIVERSITY OF BRITISH COLUMBIA

April 1989

In presenting this thesis in partial fulfilment of the requirements for an advanced degree at the University of British Columbia, I agree that the Library shall make it freely available for reference and study. I further agree that permission for extensive copying of this thesis for scholarly purposes may be granted by the head of my department or by his or her representatives. It is understood that copying or publication of this thesis for financial gain shall not be allowed without my written permission.

Engineering Physics
The University of British Columbia
2075 Wesbrook Place
Vancouver, Canada
V6T 1W5

Date: April 24 / 1989

Abstract

Thin films of the $Bi_2Sr_2Ca_2Cu_3O_y$ superconductor with T_c in excess of 106K were produced through a two step process involving rf magnetron sputtering of an oxide target followed by annealing in oxygen. The effects of various production parameters on the deposition and quality of the films were studied.

During deposition, ion bombardment of the films directly in front of the sputtering target lead to an increase in film density and to resputtering. Films from this area tended to flake off of the substrate during processing. Heating the substrate during deposition reduced the flaking problem, but caused the concentration of bismuth to drop at temperatures above 350°C.

Optimal post-deposition processing conditions were dependent on several factors including film composition, lead doping, and oxygen concentration in the annealing atmosphere. After processing, only lead doped films resulted in significant amounts of 2223 and zero resistance T_c's above 100K. The optimal initial film composition was $Pb_{1.1}Bi_2Sr_2Ca_2Cu_3O_y$. The best annealing conditions for such films were 865–875°C for 16 h in flowing oxygen.

During processing, films developed in a sequence of 2201, 2212, and, in lead doped films, 2223. The lead dopant was steadily lost during processing, and no detectable amounts remained in some of the best films after processing. Development of the 2223 phase stopped when the lead loss from the films was essentially complete.

Table of Contents

List of Tables

List of Figures

Acknowledgement

First, I must express my gratitude to my research supervisor, Dr. R.R. Parsons. Without his continual support and ready supply of ideas, this work would have foundered early. Also instrumental were the assistance and encouragement of Doug Burbidge, Brian Sullivan, and especially Norman Osborne and Peter Mulhern. I am also grateful for the constant moral support from my family and from Leslie Grant. Finally, I would like to thank the Natural Sciences and Engineering Research Council, the University of British Columbia, and Corona Vacuum Coaters Inc. for their generous financial support, as well as Doctors J. Carolan and W. Hardy for their helpful discussions and ideas.

Chapter 1

Introduction

1.1 Superconductivity

Superconductivity is a phenomenon of certain materials which, when cooled below a particular temperature called the critical temperature (T_c), lose all resistance to a direct electrical current.[1,2] In addition, while in the superconducting state, these materials exhibit the total exclusion of magnetic fields by what is called the Meissner effect. These properties are the result of a purely quantum mechanical effect which has been explained to a large extent by the famous Bardeen-Cooper-Schrieffer (BCS) theory.[3]

The superconducting state is fragile. In addition to being lost if the sample is heated above the (usually very low) critical temperature, the superconducting properties can be destroyed by being exposed to magnetic fields above the critical field (H_c) or by carrying excessive current densities (above J_c). Also, the quantum mechanically perfect zero-resistance state only holds for direct currents, so small losses (increasing with frequency) will be incurred by alternating currents.[5]

Superconductivity was first discovered in 1911 by Heike Kamerlingh Onnes in mercury. Upon cooling the metal to below 4.1 K, he observed an abrupt transition in resistance to zero. Over the next few years he discovered a number of other metals such as lead and tin which also became superconducting near 4 K. Unfortunately, this temperature is very low for practical applications, and a great deal of effort was expended by researchers over the next 75 years in an effort to raise the highest known critical temperature to

more practical levels.[4] Progress in this enterprise was very slow and as late as 1986 had reached only 23 K in Nb_3Ge.[5]

In 1986, however, a shift in the strategy from examining metals and alloys to studying oxides paid off for two IBM (Zurich) researchers. Bednorz and Muller[7] discovered that by doping a La-Cu-O compound with Ba, they could produce a superconductor with a T_c of about 30K (raised to 40K with the replacement of barium with strontium). This was the first of the so-called high temperature superconductors — the name given to all of the recently discovered ceramic (oxide) superconductors with a critical temperature above that of Nb_3Ge.

These high temperature (high-T_c) superconductors became extremely popular among solid state researchers and the mass media after the discovery in 1987 by Chu *et al*[8] of $YBa_2Cu_3O_{7-\delta}$ which had a critical temperature of about 90K — well above the boiling point of liquid nitrogen. Other high-T_c superconductors were soon found (see Table 1.1) — some with even higher critical temperatures such as $Bi_2Sr_2Ca_2Cu_3O_y$ and several of the Tl-Ba-Ca-Cu-O compounds. This abrupt change in the pace of development in superconductivity can be appreciated by looking at a graph such as Figure 1.1 which shows the rise in highest known critical temperature since Onnes's discovery.[4]

Material	Discoverer	T_c
La-Ba(Sr)-Cu-O	Bednorz & Muller[7]	30-40K
$YBa_2Cu_3O_{7-\delta}$	Chu[8]	90K
$YBa_2Cu_4O_8$	Marshall[9]	60–80K
$Bi_2Sr_2Ca_1Cu_2O_y$, $Bi_2Sr_2Ca_2Cu_3O_y$	Maeda[11]	85K, 110K
Tl-Ba-Ca-Cu-O	Hermann[12] and others[6]	up to 120K
K-Ba-Bi-O	Cava[13]	30K
Pb-Sr-Ln-Cu-O	Cava[14]	68K

Table 1.1: High-T_c materials discovered so far

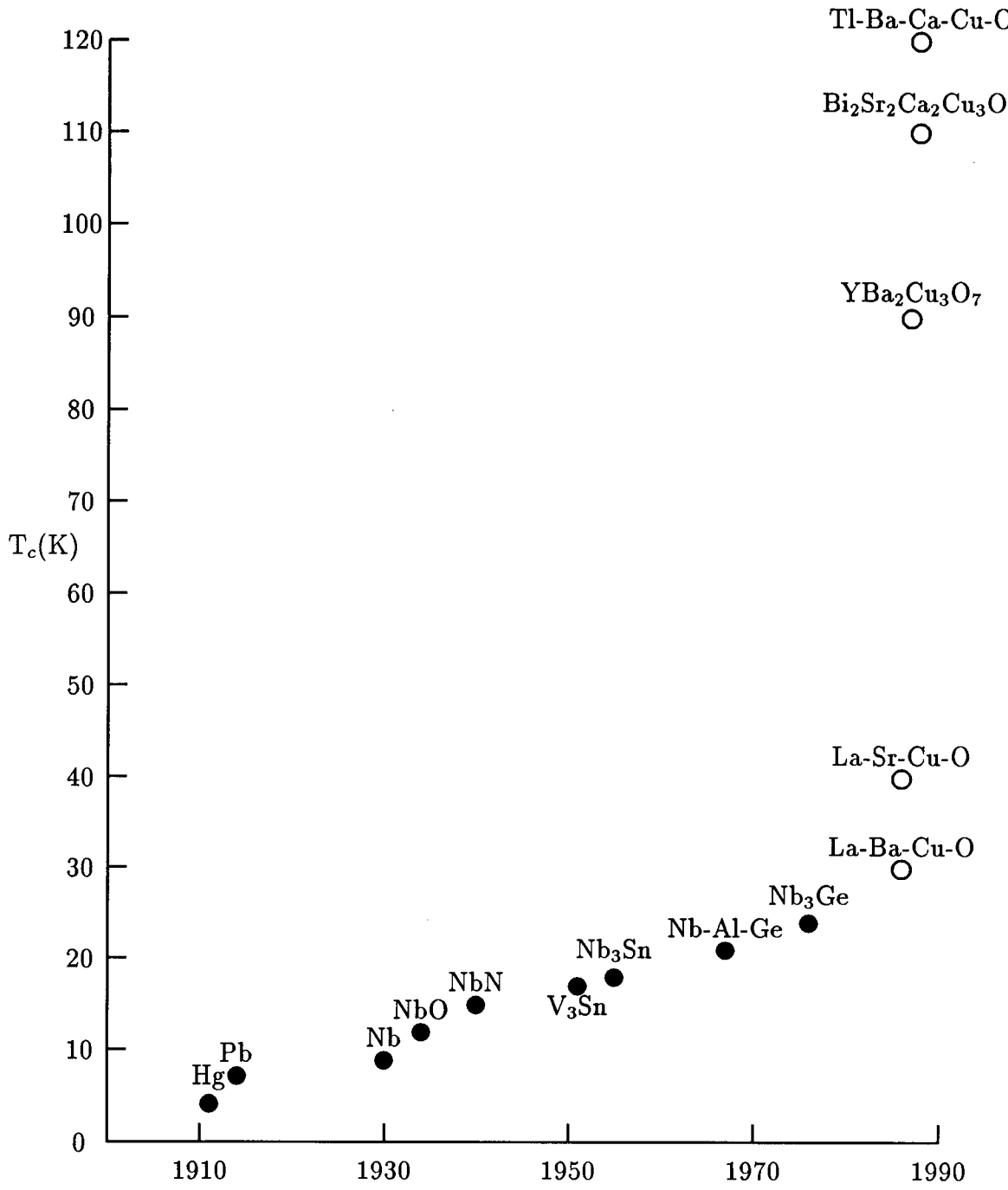

Figure 1.1: Highest known T_c over the past 75 years. Open circles indicate high-T_c Superconductors.

1.2 Potential Applications

Applications of superconductivity have been obvious since the phenomenon was first discovered. Onnes, himself, predicted that efficient superconducting electromagnets could replace iron core ones which are very heavy and limited by saturation effects.[5] In addition to electromagnets, the most important applications of superconductivity have been in magnetic levitation (the Japanese HSST), magnetic resonance imaging (medical imaging), and SQUID detectors (magnetic field measurement). Some potential or underdeveloped uses include more efficient motors, generators, power transmission, material separation, electromagnetic shielding, as well as faster electronic interconnects, signal processing, and computer elements. In addition, new devices such as energy storage rings, high frequency infrared detectors, bolometers and other sensors, and many other applications as yet unknown are conceivable.[5] Unfortunately, the extent to which this technology has been applied has been limited to a large degree by the cost and complexity of the liquid helium cooling technology that is required to maintain conventional (low temperature) superconductivity.

However, with the discovery of superconductors which have critical temperatures above the boiling point of liquid nitrogen, this refrigeration problem is significantly reduced. There are several reasons for this. The first is the relative cost of the two coolants. A litre of liquid helium is \$12.50 compared with 53 cents[1] for liquid nitrogen. Also there is the difference in efficiencies. With a heat leak of 1 W, liquid helium will evaporate at a rate of 1.4 ℓ/h compared with 0.016 ℓ/h for liquid nitrogen.[5] As a consequence of these two factors, it is necessary to provide additional bulky and expensive insulation for helium systems which increase cost and reduce flexibility for applications. As well, helium vented into the atmosphere can be permanently lost, making a recovery system

[1] 1989 prices to UBC Physics Department

obligatory. All of these factors favour the use of liquid nitrogen-cooled high temperature superconductors over conventional liquid helium ones — given all other factors being equal.

However, there are other requirements to consider aside from critical temperature. The restraints of critical current density and critical magnetic fields may delay or even prevent application of otherwise attractive materials. Low critical current densities delayed implementation of Onnes's suggestion of superconducting magnets for fifty years until the discovery of Nb-Ti and Nb_3Sn.[5] Whether application of the new superconducting materials will be limited in this manner is not yet determined, but a brief review of what has been learned so far will be given below in Section 1.5.

Several of the potential applications discussed above require special forms for the new materials. For example, the magnets and generators would likely be built out of superconducting wires. Magnetic levitation may rely on superconducting plates or shields which expel flux through the Meissner effect. Electronics and sensor applications will generally require thin film superconductors to function. As the title implies, this work will concentrate on developing this last technology — high temperature superconducting thin films.

1.3 Film Technologies

There are many different film technologies, and most of them have been applied at some time or another to produce the new high-T_c superconductors in film form. These include electron beam[15,16,17] and thermal[18,19,20] evaporation; laser ablation[21,22, 23]; ion beam,[24] triode,[25,26] and magnetron[27,28,29] sputtering; chemical vapour deposition[30]; plasma spraying[31,32]; liquid phase epitaxy[33]; spray pyrolysis[34,35]; and melt-quenching[36,37] — to name a few.

Each of these film deposition techniques has its relative strengths and weaknesses. Due to the high vacuum required and the low opportunity for contamination, it can be argued that electron beam evaporation and laser ablation would result in the best film quality. These systems, however, are relatively expensive, complicated, and have generally poor deposition rates. The thick film technologies such as spray pyrolysis and melt quenching have lower cost and higher rates but can suffer from segregation, impurities, and inhomogeneity. Sputtering, however, represents a fairly good compromise. This process combines relatively simple and flexible technology with high quality product at respectable rates. For these reasons, sputter deposition has probably been the most popular of the film technologies applied to the new superconductors.

1.4 Principles of Sputtering

By definition, sputtering occurs whenever material is ejected from the surface of a solid due to momentum transfer from a bombarding particle.[38] Sputter deposition occurs when the flux of ejected material is collected on a substrate to form a film. As mentioned above, there are different types of sputtering processes. These are generally all vacuum technologies and differ only in the technique used to generate the bombarding particles. For instance, ion beam sputtering employs an ion gun to direct charged particles into the target which is the source of the coating material.

More elegant and effective than ion sputtering are the glow discharge methods. These use a low pressure gas-discharge plasma (usually of argon) as the source of the bombarding ions. The positive plasma ions are accelerated by a negative bias potential into the target material where they cause sputtering to occur. The elegance of this approach is that additional ions are produced through collisions by secondary electrons (which are produced as a result of sputtering) moving away from the target. In this way, the plasma

is replenished with ions to continue the process.[38,39] (See Figure 1.2)

There are several types of glow discharge sputtering — of which dc and rf sputtering are the most common. In the case of the former, the negative voltage applied to the target is sufficient to sustain the discharge by the process described above. Unfortunately, this technique can only be applied to good conductors such as metals. With rf sputtering, this restriction is removed. Here, the radio frequency power applied to the target excites the argon gas to form the plasma. Because the electrons are lighter and more mobile than the positive ions, the plasma acts as a diode at rf frequencies. This results in a net negative bias voltage being formed at the target which then drives the sputtering action in a manner similar to dc sputtering.

With both dc and rf sputtering, the efficiency of the process can be enhanced with a magnetron source which produces a magnetic field in front of the target. This field serves to contain the plasma through the $\vec{E} \times \vec{B}$ drift of electrons in the presence of magnetic and electric fields.[40,39,41]

For this work, thin films of the high temperature superconductors have been produced using a rf planar magnetron sputtering source. This configuration combines relatively simple but flexible technology with fast and efficient deposition.

1.5 Properties of High Temperature Superconductors

So far, the high temperature superconductors have all been ceramic materials and are consequently quite brittle and inflexible. They are generally black and opaque, and bulk samples have tended to be porous and grainy. All of the new superconductors are based on a layered structure which, with the exception of K-Ba-Bi-O, feature one or more Cu-O layers which are believed to play the central role in producing the superconductivity.[6] The higher T_c materials, especially, are part of superconducting families — the members

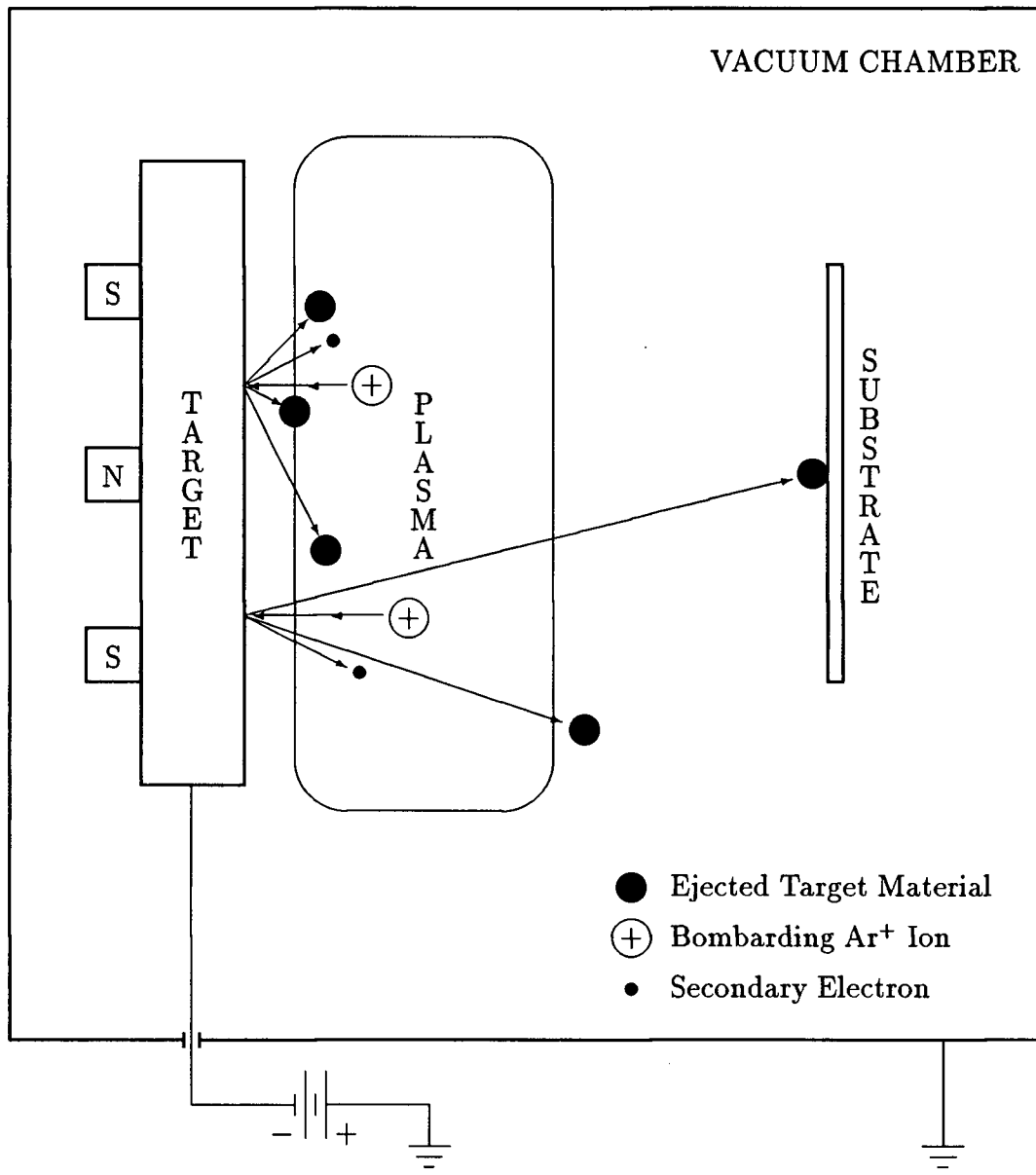

Figure 1.2: Schematic representation of magnetron sputtering. Positive argon ions are attracted to the negatively biased target. Ions striking the target eject electrons and target material — some of which coats the substrate. The electrons serve to generate more ions while the magnet arrangement enhances ion generation in front of the target.

of which differ primarily in the number of Cu-O layers present. Examples of these families include $YBa_2Cu_3O_{7-\delta}$ and $YBa_2Cu_4O_y$, $Bi_2Sr_2Ca_{n-1}Cu_nO_y$ (where n=1,2,3), and the host of compounds based on Tl-Ba-Ca-Cu-O. Due to this layered structure, these materials tend to be very anisotropic.[6]

All of these materials appear to be Type II superconductors. This means that above a lower critical magnetic field (H_{c1}) some flux penetrates the superconductor but is 'pinned' (usually by defects in the crystal) into bundles which suppress the superconductivity only in a constrained local region. It is not until the applied field exceeds an upper critical field (H_{c2}) that superconductivity in the entire sample is overcome.[1,5]

Some of the electrical, magnetic, and superconducting properties of the more important high-T_c and conventional superconductors are summarized in Table 1.2. Comparing, one can see that the coherence lengths (ξ) of the high-T_c superconductors tend to be quite small with respect to the conventional ones.[43] This poses technological problems for the creation of coherence-effect devices such as Josephson junctions. As well, even though the critical currents in single crystal films can be quite high (10^6 A/cm^2), the bulk material has values which are usually several orders of magnitude smaller. This reduction is believed to be due to defects such as porosity, grain boundaries, and tilt between grains.[43]

A further concern about the high-T_c materials is the effect of magnetic fields on critical currents. Ordinarily, applied fields will reduce the critical current density, but this effect is particularly strong in the high-T_c superconductors — despite the very high H_{c2}'s. The reason for this strong degradation in performance is believed to be a thermally activated process described as flux lattice motion [56,57]. In this process, flux bundles in a penetrated ($H_{c1} < H < H_{c2}$) superconductor are dislodged by thermal processes from their pinning centres and allowed to move to another centre. This dissipates energy and reduces the critical currents. The phenomenon of flux motion appears to be unusually

Material	T_c	H_{c1}	H_{c2}	J_c(77K)	ξ	Ref
La-Ba(Sr)-Cu-O	41K	60mT	36T	$6000_{(4K)}$ Acm^{-2}	3-5 nm	[42]
$YBa_2Cu_3O_{7-\delta}$	90	50	100	25000	2-3	[42,43]
(c-axis)					0.6	[44]
(film)				10^6		[43]
$Bi_2Sr_2Ca_1Cu_2O_y$	85	2	440	500	3-4	[43,44,46]
(c-axis)			20		0.1-0.6	[46,45,47]
(film)				10^5		[53]
$Bi_2Sr_2Ca_2Cu_3O_y$	110	2-5	500	50	2-3	[48,51,52]
(c-axis)			25			[45]
Tl-Ca-Ba-Cu-O	120	7	100	800	1.8	[48,43,54]
(film)				10^5		[43]
Nb (Type I)	9	n/a	0.2		40	[2]
Nb-Ti	9	1	14	$10^5_{(4K)}$	6	[49,50]
Nb_3Ge	23		33	$6x10^6_{(14K)}$	6	[42]

Table 1.2: Properties of some high-T_c and conventional superconductors. Anisotropy is indicated by the c-axis values, where available. The critical fields are extrapolated (T=0) values, and the critical currents are measured at 77K except where noted. Considerable uncertainty and occasionally optimism is still inherent in the values for the high-T_c materials.

significant in the high temperature superconductors both because of the greater thermal energy (due to the higher operating temperatures), and the lower coherence lengths (which reduce the pinning effectiveness).

Obviously, the applications of the high temperature superconductors will be limited by the material properties. The short coherence lengths and weak pinning are definite drawbacks, but the high critical temperatures, currents and upper critical fields of the high-T_c thin films still make them potentially very useful. The lower critical currents and inherent brittleness of ceramic materials make the bulk superconductors appear somewhat less attractive in their present form.

I chose $Bi_2Sr_2Ca_2Cu_3O_y$ for study because of its high critical temperature. At this time, the only other two serious candidates for thin film applications are $YBa_2Cu_3O_{7-\delta}$,

which has a fairly small margin of operation above liquid nitrogen temperatures, and the thallium-based compounds which have higher toxicity and are, therefore, harder to work with and less likely to be used commercially.

1.6 The Bi-Sr-Ca-Cu-O Family

The first member of the superconducting Bi-Sr-Ca-Cu-O family was discovered in 1987 by Michel *et al.*[10] This was later identified to be $Bi_2Sr_2Cu_1O_y$ and had a T_c of about 10-20K. Early in 1988, Maeda *et al*[11] reported finding two more members with critical temperatures of 85K and 110K. These were identified by Tarascon *et al*[58] to be $Bi_2Sr_2Ca_1Cu_2O_y$ and $Bi_2Sr_2Ca_2Cu_3O_y$, respectively. Tarascon also reported that the general formula for members of this family was $Bi_2Sr_2Ca_{n-1}Cu_nO_y$, where Michel had found the n=1 (2201) phase and Maeda the n=2,3 (2212 and 2223). There have been reports of even higher members of the family being produced,[59] but generally not in sufficient quantities to characterize.

Structurally, members of this family differ only by the number of Ca-Cu-O layers present in the unit cell (see Figure 1.3). The crystals are tetragonal although they often have an incommensurate superstructure in the ab-plane.[58,60] Microstructurally, samples of the 2212 and 2223 phases tend to contain very flat crystals which grow with the flat surface perpendicular to the c-axis. Within the crystals, there are often stacking faults which lead to a mixture of the member phases even within a single grain.[58,61]

Obviously, this tendency for the phases to intergrow is a problem. Pure or nearly pure 2212 samples have been produced, but making the higher T_c 2223 in single phase has been hampered by the relative stability of the 2212.[58] Several approaches to improving the amount of the 110K material have been attempted including optimizing stoichiometry,[62,63] optimizing the high temperature processing,[64,65] depositing films

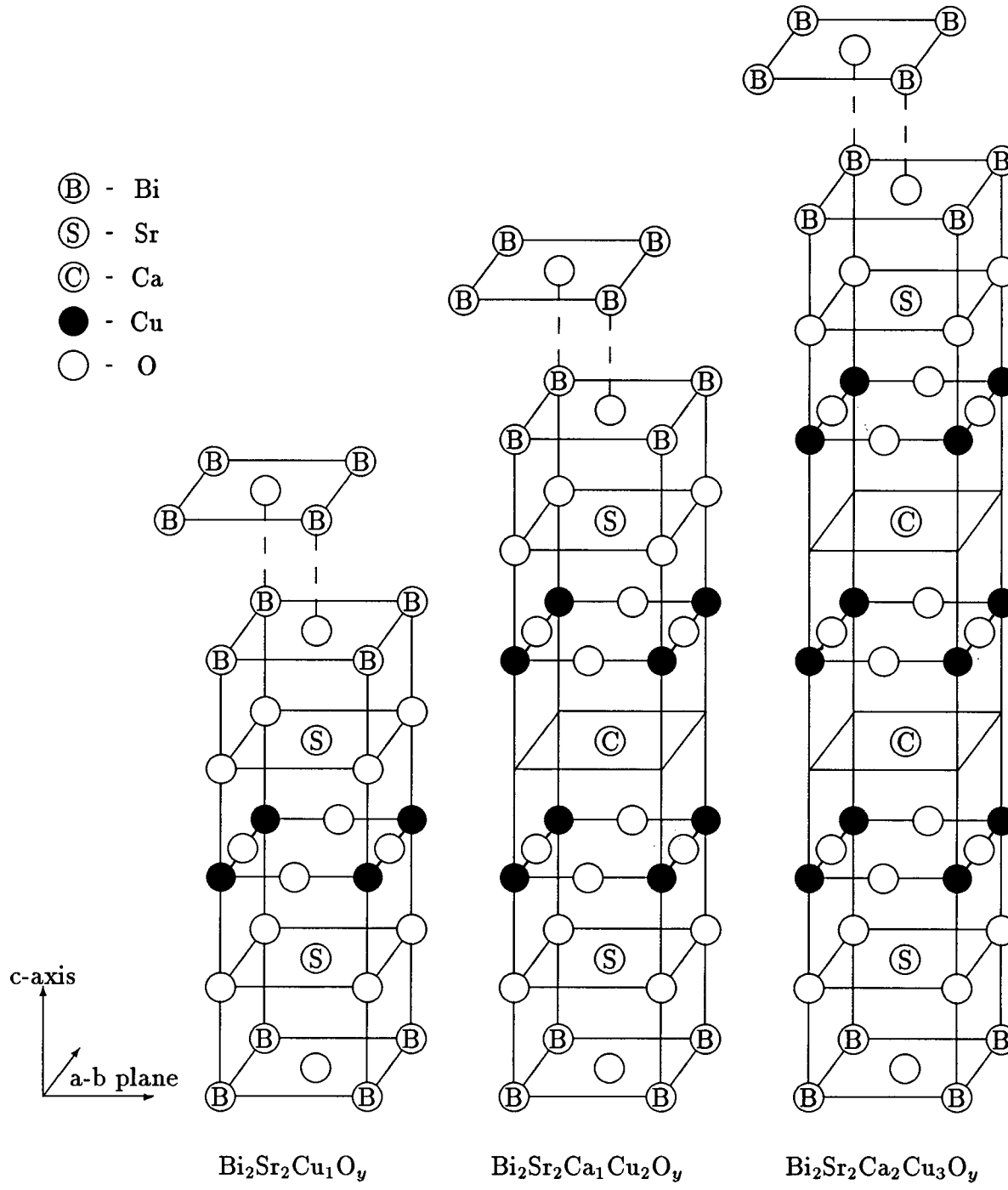

Figure 1.3: Structure of $Bi_2Sr_2Ca_{n-1}Cu_nO_y$ unit cell. Only half of the cell is shown. The other half is identical and stacks on top of the first in a manner indicated by the dashed lines.

onto heated substrates,[29] and elemental substitution.[66,68,69] All of these had little or mixed success until Sunshine *et al*[66] tried to partially substitute lead for bismuth. The addition of lead to the Bi-Sr-Ca-Cu-O system has been very effective at increasing the proportion of the 2223 phase present. In fact, several researchers have reported essentially pure 2223 samples.[70,71] However, the mechanism by which the lead aids this enhancement of the 110K phase is still not understood.

1.7 Thesis Objective

The objective of this work is to produce and characterize thin films of the $Bi_2Sr_2Ca_2Cu_3O_y$ superconductor. The motivation for this work is the ultimate production of useful devices based on high-T_c superconducting thin films. The approach chosen to produce the films is a commercially feasible one involving magnetron sputtering of an oxide target, followed by post-deposition annealing.

The organization of this work is as follows. Details of film production are discussed in Chapter Two. Once produced, the films are characterized using several techniques which are discussed in Chapter Three. The effects of varying production parameters as well as an overall characterization of the superconducting films are given in Chapters Four (depositional effects) and Five (processing effects), and Chapter Six presents the conclusions of this study as well as the recommendations for further work.

Chapter 2

Film Preparation

2.1 Introduction

In general, preparing high temperature superconducting thin films involves two steps — deposition and post-deposition processing. The latter is necessary because films deposited at or near room temperature are amorphous and insulating. (Bi-Sr-Ca-Cu-O films deposited onto heated substrates have been reported to be superconducting, but so far their properties have been inferior.[29,72]) A high temperature step is required to cause the growth of the superconducting crystal structure. The superconducting properties of the film are highly dependent on this processing step.

This chapter is divided into two parts. The first deals with the details and apparatus involved in the sputter deposition of Bi-Sr-Ca-Cu-O films. The second part discusses the parameters and equipment relevant to the post-deposition processing.

2.2 Deposition

Both the apparatus and the procedures used to deposit the unprocessed films are discussed in this section. The apparatus described includes the sputtering system, the targets which provide the coating materials, and the substrates upon which the films grow. The description of the sputtering procedures gives details of the deposition conditions used and some explanation of why they were chosen.

2.2.1 Sputtering System

A sputter deposition system is composed of a vacuum chamber, sputtering sources, a power supply, and a variety of attendant instrumentation.

A diagram of the vacuum system used is given in Figure 2.4. It consists of a cylindrical steel chamber which is evacuated by a standard rotary pump and diffusion pump configuration. A liquid nitrogen cold trap is used to prevent the pump oil from backstreaming into the chamber. The quality of the vacuum is determined by the lowest, or base, pressure which the system can obtain. For the system used, this was determined using an Varian ion gauge to be $5–10\times10^{-6}$ Torr.

During deposition, the diffusion pump was throttled by partially closing an entrance baffle. This served to increase the argon pressure without excessively loading the diffusion pump. Deposition pressures were monitored using an MKS Baratron.

There were four 2 inch diameter sputtering sources mounted inside the chamber. All of these were water-cooled magnetron sources. Three of these were Corona[1] – 2" sources and the fourth was an US-Gun which was only suitable for dc sputtering. Generally only one source was used at a time in these studies, but occasionally a film was prepared which was a mixture of two different targets.

Substrates were mounted on a turntable which was directly in front of and 7.8 cm (4.5 cm if the substrate heater was used) from the surface of the sputter target. Frequently, the films were deposited off of the main axis (See Figure 2.5) of the discharge to avoid bombardment effects (which are discussed in Chapter Four). When the film was being produced from multiple targets, the table was rotated by a stepper motor between the active sources. A shutter was situated between the substrate holder and the sources to allow the targets to be presputtered (cleaned) before actual deposition. However, the

[1]Corona Vacuum Coaters Inc., P.O Box 46662, Station G, Vancouver, B.C., V6R 4K8

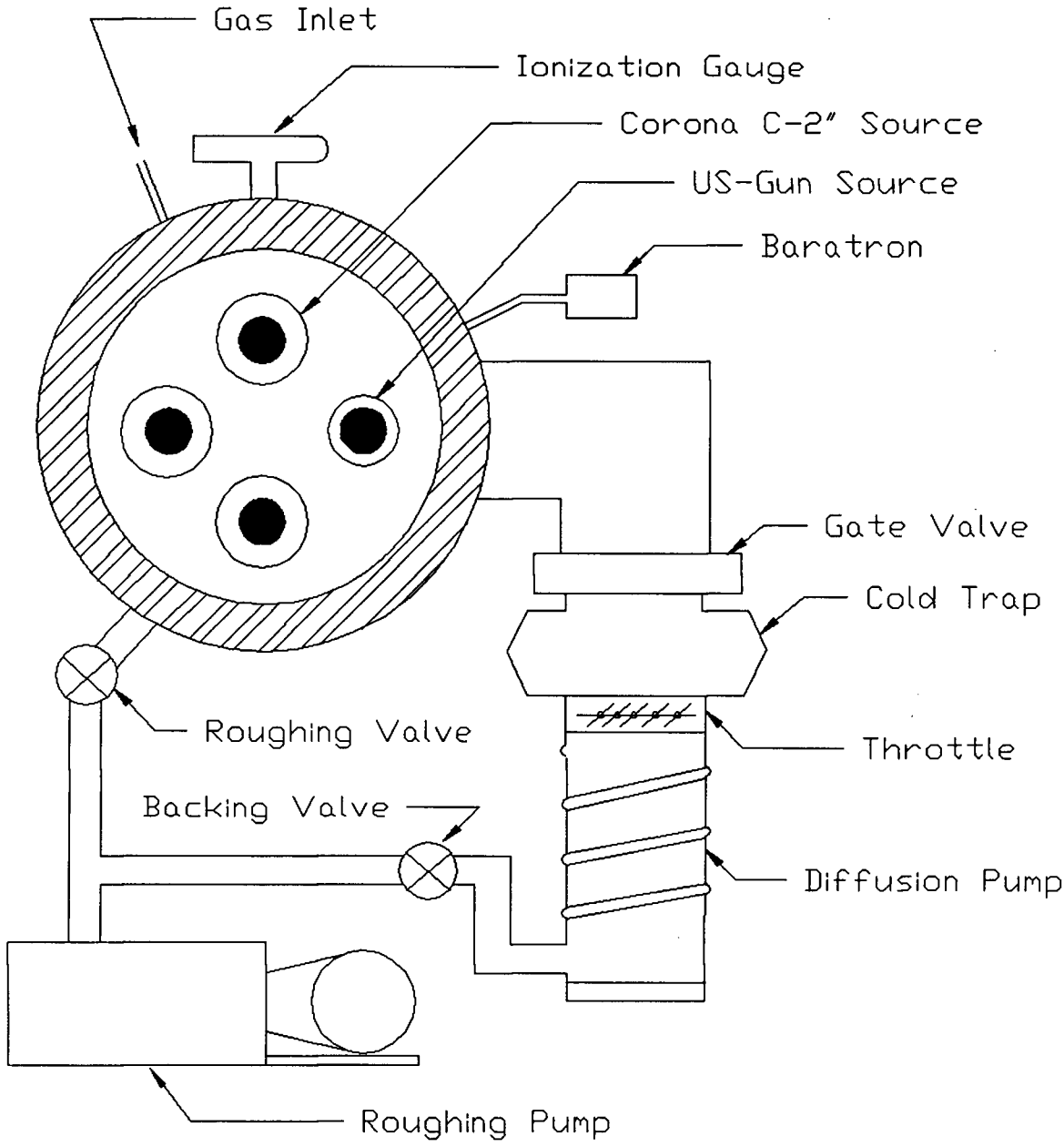

Figure 2.4: Diagram of the sputtering system. The view is of the front with the door, table, and shutter removed.

shutter could not be used in conjunction with the substrate heater.

In some experiments, the substrates were instead mounted on a substrate heater which consisted of a stainless steel block with an imbedded 85W cartridge heater. The edge of the substrate was clamped to the block using a crystal of MgO to enhance thermal contact.

Due to rf inductive effects, temperature could not be monitored during the film deposition. Instead, the substrate temperature was calibrated to $\pm 10°C$ against heater power (with the discharge off) using a chromel-alumel thermocouple attached to the exposed substrate surface with silver paint. This calibration ignored the heating effects due to bombardment during deposition; however, damage to cellophane tape holding room temperature substrates indicates this heating was only of sufficient power to raise the temperature of the films to 50–75°C. At a substrate temperature of 600°C, this amount of power would only raise the temperature an additional 1–3°C, and could be neglected.

Sputtering power was supplied by either a Plasma-Therm 5000W dc supply, or an Energy Research Associates HFP 8000 rf (13.56 MHz) supply which was signal-matched to the source using a load matching transformer. For reasons discussed below, the rf supply was primarily used.

2.2.2 Target Fabrication

The targets which provided the film material were disks 50 mm in diameter and 3–4 mm thick. They were formed from reacted and pressed powders of the constituent metals' oxides and carbonates. The raw materials for the targets were powders of high purity (usually 99.999%) Bi_2O_3, $SrCO_3$, $CaCO_3$, CuO, and PbO. These were mixed in the appropriate cation ratios and typically fired in air at 780°C for 12 hours, cooled, and then mechanically reground in an agate mortar. The firing and regrinding was repeated

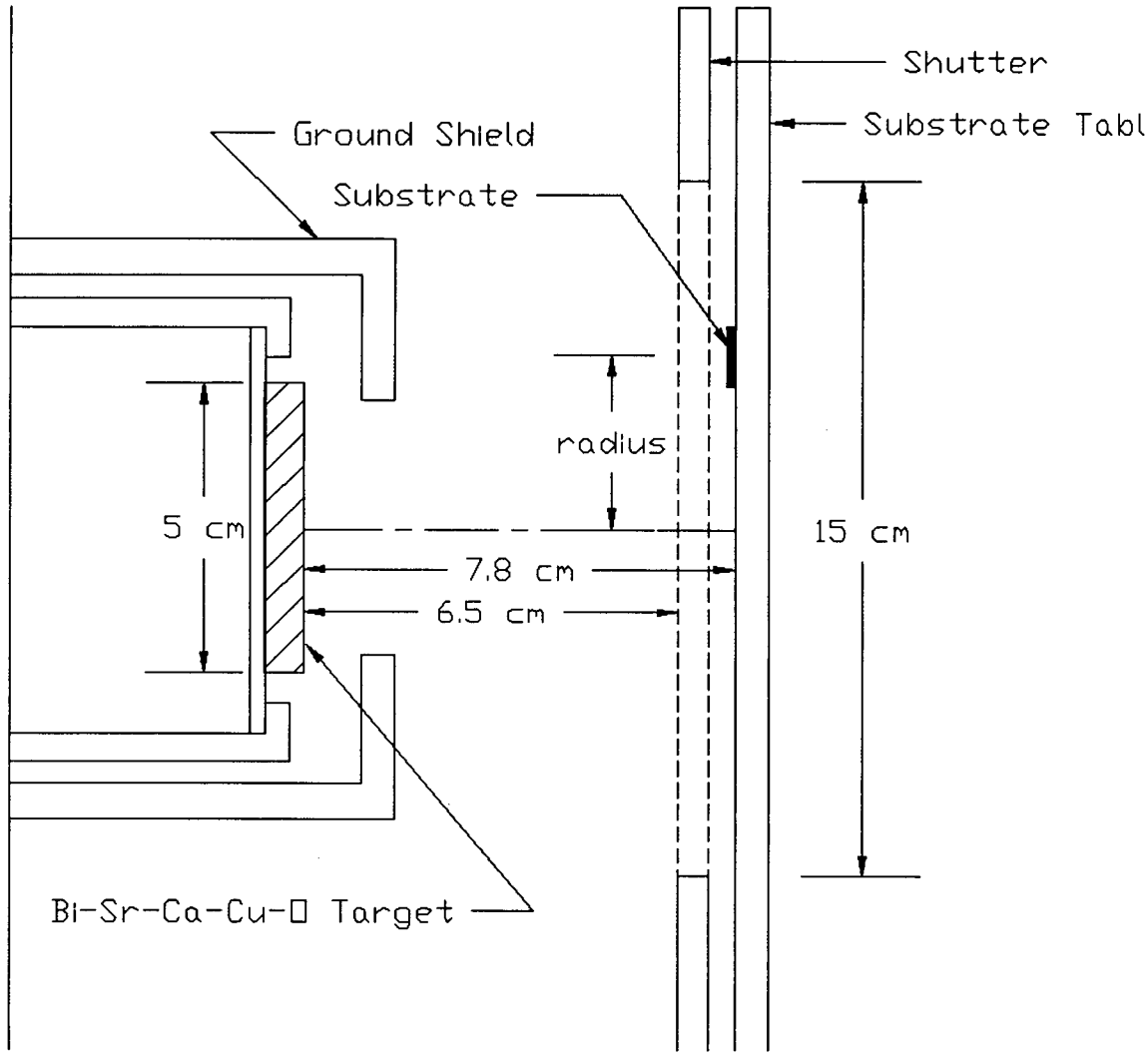

Figure 2.5: Deposition geometry. The shutter is in the open position. The radius of a film deposited off of the main axis is indicated.

at 790°C and 795°C. The mixtures were then pressed into disks at 1.4 kbar and sintered at 825°C for 12 hours. The repeated firings and final sintering were necessary in order to form strong, homogeneous, and well-reacted targets.

The nominal compositions of the targets used are given in Table 2.3. These targets are identified in the following chapters using the TBn labels shown. Also in this thesis, target or film compositions are described using a ratio of metal atoms in the sequence Bi:Sr:Ca:Cu. If lead is present, it is included in parentheses before the bismuth concentration — such as (1.3)2:2:2:3. References to particular phases that have fixed molecular structure but are identified by their composition, are given without colons — such as 2223.

Target	Pb	Bi	Sr	Ca	Cu
TB3	-	2	2	1	2
TB5	-	4	3	3	4
TB7	-	2	2	2	3
TB8	-	4	3	3	5
TB9	1	1	2	2	3
TB10	2	2	2	2	3

Table 2.3: Cation compositions of targets used

For mounting in the source, the finished targets were sanded flat and attached to copper backing plates using silver epoxy. This arrangement was necessary to provide good thermal conductivity from the target, where considerable heat is generated during sputtering, to the backing plate which was clamped into the source and water-cooled.

2.2.3 Substrate Preparation

Few substrate materials are appropriate for superconducting $Bi_2Sr_2Ca_2Cu_3O_y$ films because they must be able to withstand an oxygen atmosphere for extended durations at

high temperatures during the post-deposition processing. More stringently, they must not react with any of the elements in the film under these conditions. So far only $SrTiO_3$ and MgO have been used successfully as substrates for Bi-Sr-Ca-Cu-O films. Due to the relative costs involved, most of the films made for this work were deposited onto MgO. Single crystal substrates were used to promote epitaxial growth. These were cleaved by the supplier to the approximate dimensions of 10x10x1 mm with the flat surface perpendicular to the (100) crystal orientation. The crystals were usually cut further into halves or thirds.

Other substrates such as Corning 7059 glass and quartz were used for characterization of the as-deposited films but could not be used if the film was to be annealed due to film-substrate reactions.[27]

Prior to deposition, the substrates were cleaned using a combination of trichlorethylene, acetone, methanol, and compressed nitrogen gas. The substrates were then mounted in the chamber using double-sided adhesive tape (unless the substrate heater was used in which case they were simply clamped in place).

2.2.4 Deposition Conditions

The ideal deposition conditions would result in fast, reproducible, uniform, and homogeneous film growth. The conditions described below were chosen with these requirements in mind. How well these criteria were satisfied will be the subject of Chapter Four.

Initially, dc sputtering was attempted with this apparatus to produce Bi-Sr-Ca-Cu-O films,[27] but difficulties with discharge stability and reproducibility prompted a switch to rf sputtering. Radio frequency sputtering resulted in a very stable plasma and uniform erosion of the target (within the ring caused by the magnet arrangement).[74]

Power levels ranged from 40 – 100 W with generally less than 3% reflected power. The target bias voltage varied with the target (discussed in Chapter Four), but was generally

seen to rise steadily for the first 15 minutes. For this reason, the target was presputtered for 15 minutes before opening the shutter to begin deposition.

Deposition was usually carried out in pure argon. (The effects of adding oxygen will be briefly discussed in Chapter Four.) The standard operating pressure chosen was 0.5 Pa which was low enough that the rate was not significantly reduced by scattering, but high enough to be used consistently without problems with discharge stability.

Deposition rates varied between targets, but the settings described above led to depositing between 7 and 15 nm/min. Total deposition time was usually 2 hours which led to film thicknesses on the order of one micron.

2.3 Processing

Post-deposition processing involves annealing the film at 800 – 900°C in a carefully controlled environment. Unfortunately, it is very difficult to optimize this critical step because the details of the reaction are not very well known. Given the complexity of the system, it would not be surprising if the optimum annealing procedure involves a complicated series of temperature ramps, dwells, and atmosphere changes. To systematically determine such a procedure would be an immense undertaking and was not necessary to achieve the thesis objective of finding a practical technique for producing superconducting $Bi_2Sr_2Ca_2Cu_3O_y$ films.

Instead, a very simple annealing procedure was used. This involved ramping temperature from ambient to some fixed process temperature and leaving it there for some time before ramping down again. The important variables are then the ramp rates, the process temperature, the annealing duration, and the atmosphere (including pressure) present in the furnace. The effects of each of these are dealt with in Chapter Five. This section describes the apparatus and procedures used for processing the films.

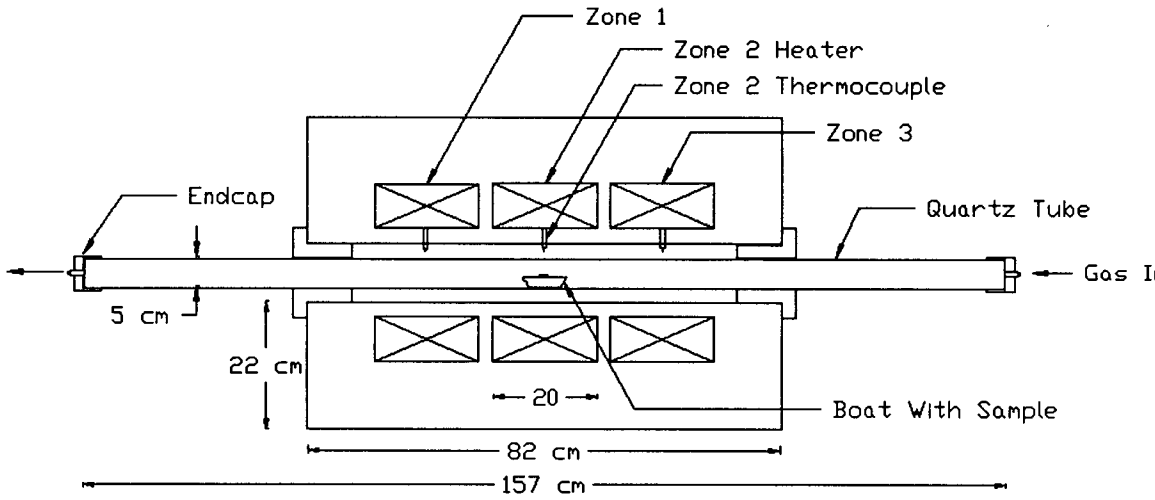

Figure 2.6: Three Zone Tube Furnace

2.3.1 Annealing Apparatus

The annealing apparatus must provide a well controlled environment and temperature. A clean environment is required because of the high temperature of the processing step and the reactivity of the film constituents. The total film material is usually less than a milligram, so even a small amount of contamination can destroy the properties of a film. In addition, the reaction is very sensitive to temperature and to the annealing atmosphere.

A tube furnace (Lindberg 55347) was used in order to maintain such exacting control over the annealing conditions (see Figure 2.6). Oxygen gas was introduced at controlled flow rates at a slight overpressure at one end of the quartz tube and vented out the other at atmospheric pressure. After loading the sample in the tube, the system was flushed with argon prior to annealing. An alternative arrangement was to remove the tube endcaps and expose the system to air.

Temperature control was maintained using a programmable three zone feedback control which was calibrated against a chromel-alumel thermocouple. A steady state error of less than 0.2°C was maintained by the controller, but due to the separation between the thermocouple and the sample, fluctuations in sample temperature of perhaps 1°C were possible. Ramp rates of up to 20 °C/min were easily maintained during heating; however, the maximum cooling rate was lower than this at temperatures below about 500°C due to the thermal time constants of the furnace.

Samples were placed film side up on a flat piece of alumina which sat on an alumina boat. The boat was inserted and removed from the tube using a stainless steel rod and hook.

Chapter 3

Analysis Techniques

3.1 Introduction

In order to develop a technique for producing high quality superconducting films, useful methods for characterization had to be found. The four point probe was an obvious direct probe for determining critical temperatures and current densities. X-ray diffraction is very useful for determining crystal growth, orientation and phase identification. The electron microprobe was a good quantitative probe for compositional analysis, and the profilometer was an important tool for determining depositional characteristics. With the use of these techniques, it was possible to test films for superconductivity and to provide information on how to improve the process for producing them.

Each of these four probes is discussed in this chapter with the description, limitations, and performance characteristics of the specific equipment used. They are presented in the sequence in which they would be typically used.

3.2 Profilometer

After deposition, film thickness and surface roughness were measured using a profilometer. This was necessary to provide information about the deposition rate and about the surface quality of the film before further processing. This allowed deposition-dependent properties of the processed films to be isolated.

The profilometer, a Tencor Alpha-Step 200, functions by dragging a needle across a

relatively flat surface to obtain a vertical profile through sensing the height of the needle. By comparing the height of the bare substrate to that of the film, the film thickness is determined. The sensitivity of this instrument was approximately $\pm 0.01\mu$m and the horizontal travel up to 2 mm.

The substrates were partially masked by cellophane tape during deposition. After removing the mask, the samples were cleaned with propanol to remove any remaining adhesive. Film thicknesses were measured by dragging the profilometer needle over the step between the bare substrate and the film. Masking did affect the film thicknesses through accumulation and shadowing, but by using the film levels far (1 mm) from the mask, these effects were minimzed.

Profilometry of the bare MgO substrates indicated that they were rough on a scale which was comparable to the film thicknesses. (See Figure 3.7 for the profile of a relatively smooth example) This was generally due to steps where the crystal had not cleaved along a single plane. Because of this roughness, smoother substrates such as glass or quartz were used when measuring thicknesses of unannealed films. It was difficult to obtain reliable thickness measurements of annealed films because both the substrate and film surface were usually too rough.

3.3 Microprobe

The electron microprobe gives quantitative compositional analysis for most elements. This is essential information because the purity of the $Bi_2Sr_2Ca_2Cu_3O_y$ thin films is quite sensitive to their composition.[63] Due to its high spatial resolution, this instrument also gives valuable information about the degree of homogeneity of the as-deposited and annealed thin films.

The microprobe system used was a Cameca SX-50 Model which operates by detecting

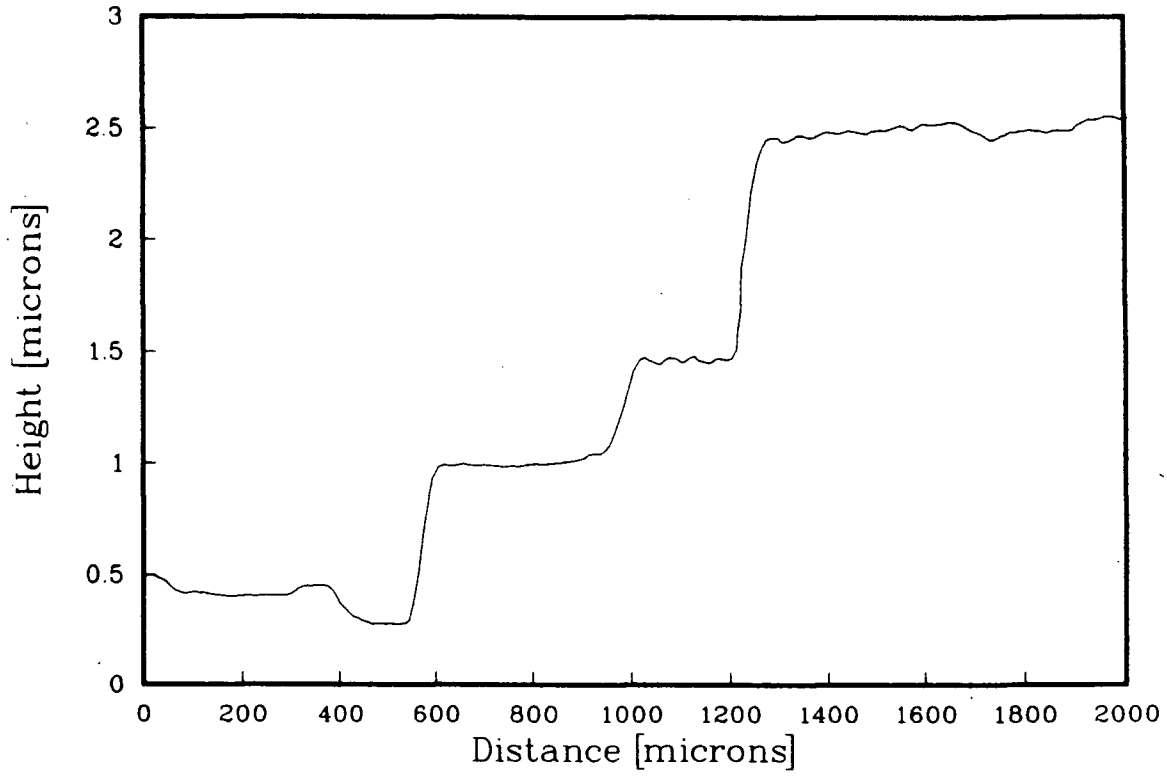

Figure 3.7: Profile of a MgO substrate showing steps in the surface height. The graph origin is arbitrary.

characteristic X-ray energies from electron beam-excited atoms. Emission intensities at specific wavelengths are monitored and compared against standards. A broad spectrum is not scanned; therefore, the microprobe only detects those elements it is programmed to look for. For this reason, Energy Dispersive X-ray (EDX) spectroscopy is often also performed in conjunction for the initial elemental identification. A SemCo Nanolab 7 scanning electron microscope equipped with a Kevex 7000 EDX system was used for this.

The microprobe used could easily detect any of the cation materials used in the

Bi-Sr-Ca-Cu-O films, but it was not always possible to determine accurate oxygen concentrations. For this reason, none of the analyses discussed in Chapters Four and Five have included oxygen determination.

Typically, the microprobe was used to analyze point samples (about 1 μm^2 spot size). The uncertainty in cation concentration for each sample was approximately 1% of the total composition. However, variation between adjacent sampling points could be much higher. For the annealed films, in particular, it was observed that the composition detected could vary significantly over a few microns. Under these circumstances, several sampling points were used for each film and a standard error computed.

The electron beam can penetrate on the order of a micron, so for films thinner than this, the substrate atoms were also excited. This increased the noise levels and decreased sensitivity. This unwanted excitation could also affect detection of specific elements if there was an overlap of atomic emission lines or if the substrate contained the same atoms as the film. Neither of these factors are believed to be important for detecting the metal atom concentrations for the current substrate and film materials.

3.4 X-ray Diffraction

In order to produce the $Bi_2Sr_2Ca_2Cu_3O_y$ superconductor, it is necessary to obtain the correct atomic structure as well as stoichiometry. X-ray Diffraction (XRD) is a simple and direct probe of this structure. By examining the patterns in an XRD spectrum one can determine information about the crystal lattice, its orientation, and about which other phases are present.

X-ray diffraction involves reflecting monochromatic X-rays off of a crystal lattice (See Figure 3.8) and determining the angles for which the Bragg Law ($\lambda = 2d \sin\theta$) for constructive interference holds. This is done by scanning the detector and source together

and recording the intensity of the reflected beam against the angle 2θ. This results in a characteristic pattern of intensities from which the crystal structure can be inferred.

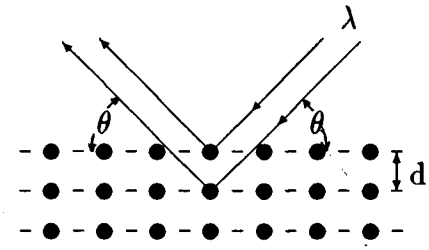

Figure 3.8: X-ray diffraction by a crystal lattice. The condition for constructive interference between X-rays reflected off crystal planes with spacing d is the Bragg Law: $\lambda = 2d \sin\theta$

By identifying these patterns, one can determine which phases are present in the sample. This technique can also give information about the orientation of crystal growth within the sample by comparing the pattern belonging to a particular phase to its random powder pattern. Since — as mentioned in Chapter One — these materials have anisotropic properties, information about the orientation of the sample can be very important.

The X-ray Diffractometer that was mainly used was a Philips system (Goniometer number PW 1050/65 D2414). The radiation was CuKα X-rays with a wavelength of $\lambda = 1.54$ Å. The detector was scanned over 2θ at $2°/\text{min}$ with an electronic time constant of 1 second. Reproducibility of this system under these conditions is estimated to be within 0.1 degree for values of 2θ. In addition, the system was periodically calibrated against a silicon standard. However, mounting restrictions could put the sample off the axis of the goniometer by up to to several tenths of a millimeter which introduced offsets in the spectra of up to 0.25°. This was of little importance for pattern recognition, but made accurate measurement of lattice spacings difficult.

In general, the films produced for this work were highly oriented. The crystals tended

to grow with their c-axis perpendicular to the substrate. This resulted in very high intensities for certain diffraction peaks in the aligned samples, but it also meant that the peak intensities were very sensitive to minor shifts in sample orientation. This sensitivity increases the uncertainty in quantitative comparisons between phases which may be oriented differently.

Some additional information can be obtained about the degree of orientation using a pole-curve (rocking curve) apparatus. This operates on the same basic principles but involves rotating the sample with the detector and source positioned for a fixed value of θ. The equipment to do this was an older Philips system (PW 1964/20 DY2030) which was more difficult to use and produced results which were ambiguous in interpretation. As a consequence, it was used sparingly.

3.5 Four Point Probe

The most important property of superconducting thin films for many applications is the zero electrical resistance. Therefore, it is necessary to determine the resistance behaviour of the films at low temperature. The apparatus used to perform this measurement was the four point probe.

The four point probe measures the resistance of the sample by passing a current between the outer two contacts (points) and measuring the resulting voltage drop between the inner two. Because very little current flows in the voltage sense leads, the voltage drop due to the contact resistance is negligible. For this system, the four points were colinear and spaced 2mm apart.

Since even high temperature superconductivity takes place at 'low' temperatures, the four point apparatus must be used in a cryostat. A liquid helium-cooled system was used for this work. This consisted of a stainless steel tube 115 cm long and 1.2 cm in diameter

which could be inserted into a standard UBC Physics liquid helium dewar. The bottom 15 cm of the tube where the sample and temperature sensor were located was made of copper to enhance the temperature uniformity. The tube was evacuated and backfilled with helium gas as a heat exchange gas at perhaps a tenth of an atmosphere.

The sample was mounted on a copper block at the end of a steel rod which fit down the centre of the tube (contact with the tube walls is minimized to reduce temperature gradients). The temperature of the sample was monitored by a silicon diode which was imbedded in the copper block. The diode was calibrated (from 25K to 325K) against a platinum resistor (Lakeshore PT-103) and this calibration verified using the vapour pressure - temperature relation of liquid oxygen. The precision of the calibration was ± 0.25K, but due to drift in the instrument, an overall uncertainty of about 0.5K is probably more reasonable.

Four point resistance was measured using one of two systems. The first was a dc system (UBC Physics Electronics Shop model 87-033-5) while the second was a low frequency ac system (97 Hz supplied by a Data Royal F210A function generator) with a lock-in amplifier (EG&G 5204). Both systems collected data with a microcomputer-controlled data acquisition system.

The performance of these two systems depended substantially on their settings (current, gain, time constants, etc.) which varied between samples. However, for a typical high quality film with room temperature resistance of about 3 Ω, the dc system (100μA current, 5000 gain) had a resolution of 0.3mΩ and a typical system noise level of 7mΩ. The ac system (50μA current, 4000 gain) had a resolution of 0.8mΩ and noise level of about 1mΩ. Translating these values into resistivities yields noise levels on the order of 1 and 0.1 $\mu\Omega$-cm for dc and ac, respectively.

Both of these four point systems suffered from some systematic error. The dc technique resulted in a small but definite linear background signal which was believed to

be due to a thermocouple effect. This was only noticeable when using the high gains needed to measure samples with the lowest normal state resistances. The ac apparatus resulted in very flat baselines, but reactance effects in high resistance samples resulted in anomalous negative-resistance signals. Since neither system (ac or dc) was ideal, but they had complementary advantages (ac for low resistances, dc for high), both were used for four point measurements.

An important measurement made using the four point probe is that of the critical current of the sample. This was estimated by increasing the current to the superconducting sample until the voltage between the inner points rose above a threshold value (usually $1\mu V/cm$). Unfortunately, contact resistance to the samples was quite high and may have caused warming of the sample at higher currents. This could be minimized by necking the film down between the contacts so that the critical currents were small (although the density may have been quite high).

Substrate roughness was an additional impediment to measuring a representative critical current for a sample. Since (as seen in Figure 3.7 above) the substrates have steps which can be as large as the film thickness, poor continuity could arise in films which are of otherwise high quality. The anisotropic nature of these layered materials makes this problem worse since the grains in the tilted sections of the film connecting the steps will be poorly aligned which will considerably reduce critical currents. Dimos *et al*[73] found with epitaxial films of $YBa_2Cu_3O_{7-\delta}$ that critical current density drops by an order of magnitude if there is a misorientation of just 10° between grains. Since Bi-Sr-Ca-Cu-O superconductors are even more anisotropic than $YBa_2Cu_3O_{7-\delta}$,[46] this reduction of J_c is likely to be even worse for the $Bi_2Sr_2Ca_2Cu_3O_y$ films considered in this work. Consequently, any critical current measurements made of films on MgO substrates of this nature will be a significant understatement of the material's intrinsic capability.

Chapter 4

Characterization of Deposited Films

4.1 Introduction

This chapter discusses the characterization of the as-deposited Bi-Sr-Ca-Cu-O films. A description of a representative film is presented first, followed by a discussion of its features and their consequences for possible applications. Following this, the effects of varying the deposition parameters of substrate temperature, sputtering atmosphere, and target composition are discussed.

Deposition of Bi-Sr-Ca-Cu-O thin films for superconductor applications would require reproducibility, control, and uniformity of composition, thickness and texture. In addition, it would be necessary that the films have sufficient adhesion to the substrate so that they do not separate during processing. The system and procedures described in Chapter Two for producing the films for this work satisfy most of these criteria, but with certain reservations. The most serious problems discovered so far are compositional fluctuations due to substrate temperature or position, and ion bombardment during deposition leading to the flaking of the film in the processing stage. These factors are discussed below.

4.2 As-Deposited Bi-Sr-Ca-Cu-O Films

Most of the Bi-Sr-Ca-Cu-O films deposited at room temperature had a similar appearance. They were amorphous with a smooth, glassy texture. Films which were deposited

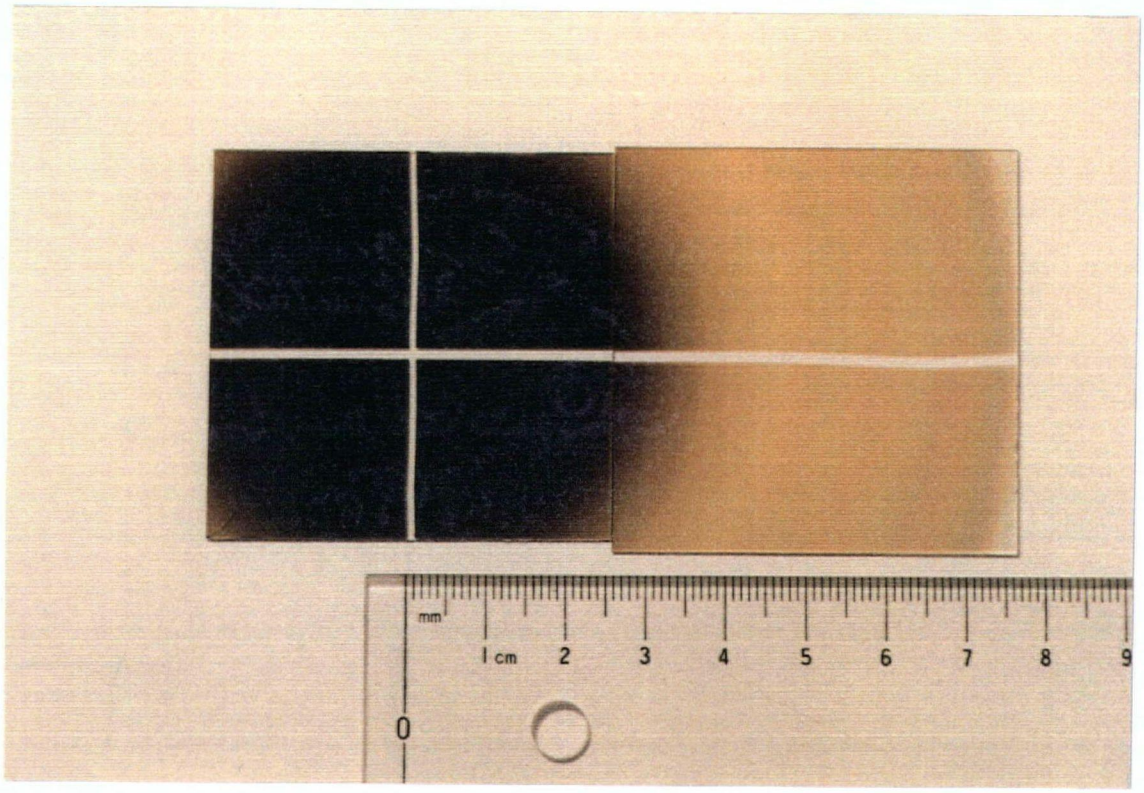

Figure 4.9: Photograph of an as-deposited Bi-Sr-Ca-Cu-O film. The cross pattern is a result of masking the substrate for profilometry and indicates the centre of the discharge.

directly in front of the target (centred on the axis of the discharge) often had a few small pits in the film. However, these pits were absent in films deposited a few centimetres away from the centre of the discharge axis. Looking from the centre outwards, the films underwent a significant change in colour at a radius of 2.5 – 3 cm. The transition was from a dark opaque brown directly in front of the target to a lighter transparent yellow (See Figure 4.9 for a photograph).

The appearance of these films suggested that they were thickest in the center and tapered off towards the edges, as would be expected for a typical sputter-deposited film. However, the profile of the Bi-Sr-Ca-Cu-O film shown in the photograph above indicates (Figure 4.10) that it was actually thickest 2.5 cm away from the centre, near the point where the film colour changed.

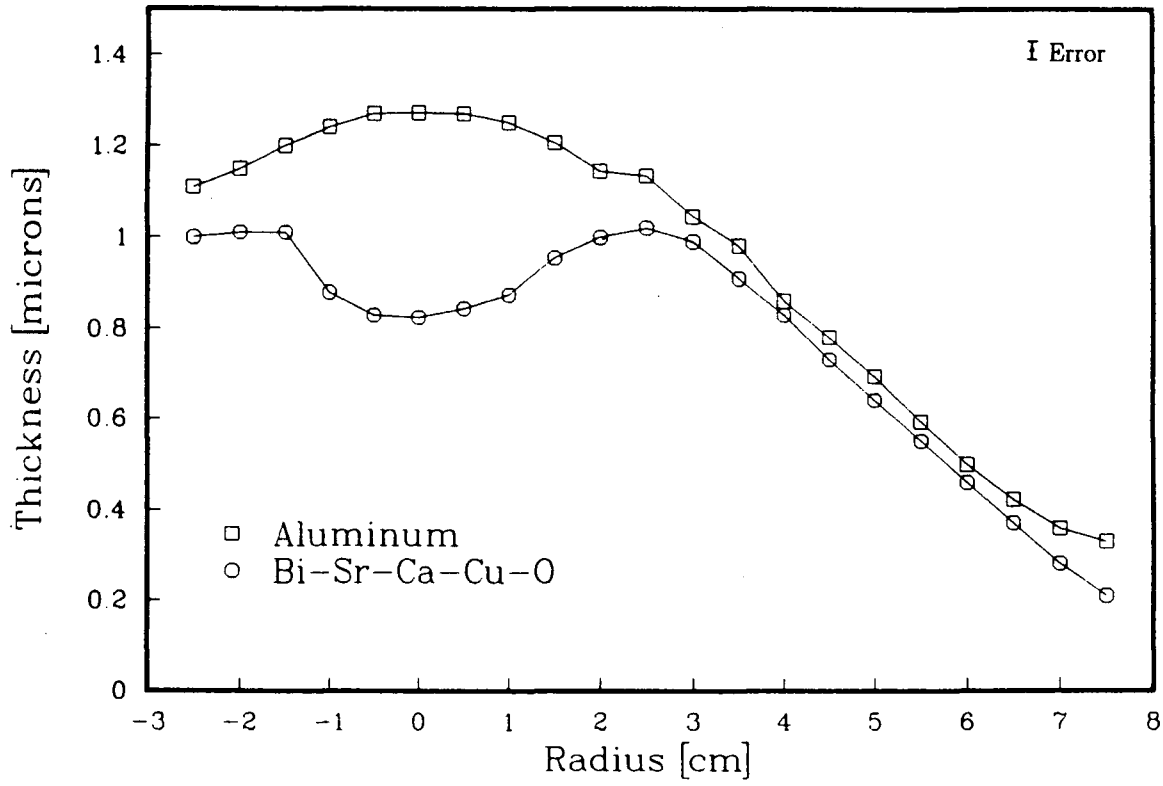

Figure 4.10: Thickness profile of a Bi-Sr-Ca-Cu-O film (2:2:2:3) with an aluminum film deposited under the same conditions for comparison. The graph covers the same region as Fig. 4.9

There were compositional variations across the useable film area as well. In the centre, the films tended to be rich in copper whereas they were deficient in that element further out. The other elements were present in close to stoichiometric amounts. (See Figure 4.11) Targets which contained lead (TB9 and TB10) resulted in films which were uniformly below nominal stoichiometry in lead. This is believed to be due to a loss of lead in the target itself during sintering. This possibility is supported by results presented in Chapter Five. Due to this loss, films produced from target TB10 were approximately 35% below nominal stoichiometry in lead. Nominal lead compositions of TB10 films reported below have already been corrected for this factor.

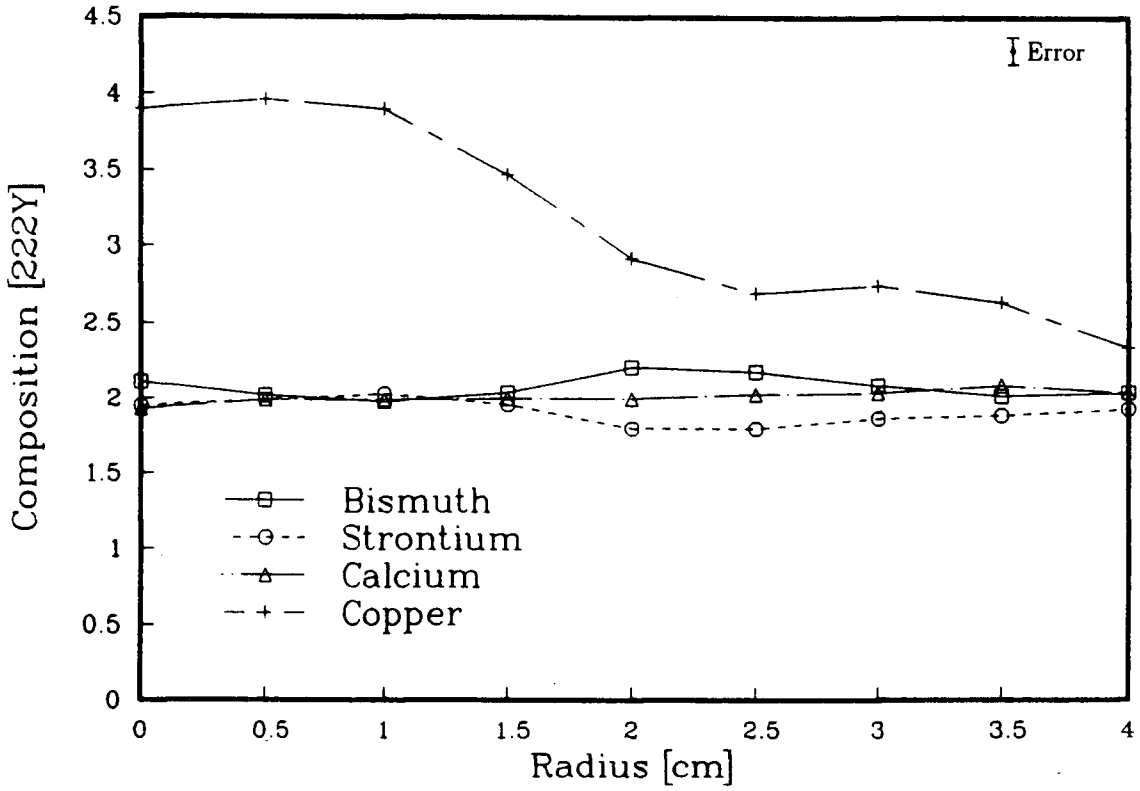

Figure 4.11: Variation in composition away from the centre of the discharge. Nominal composition is 2223.

4.3 Ion Bombardment

The two films of Figure 4.10 were deposited under nearly identical conditions. They were sputtered from the same source with the same target-substrate separation, sputtering pressure, and rf power. Yet their respective profiles are very different. A possible explanation for this difference is that the Bi-Sr-Ca-Cu-O target generated negative ions during sputtering. These ions would have been accelerated away nearly perpendicular to the target due to the interaction of their charge with the bias voltage.[78] These particles would subsequently have bombarded the film directly in front of the target, thereby altering its profile.

Several observed features are consistent with this hypothesis. First, there is the

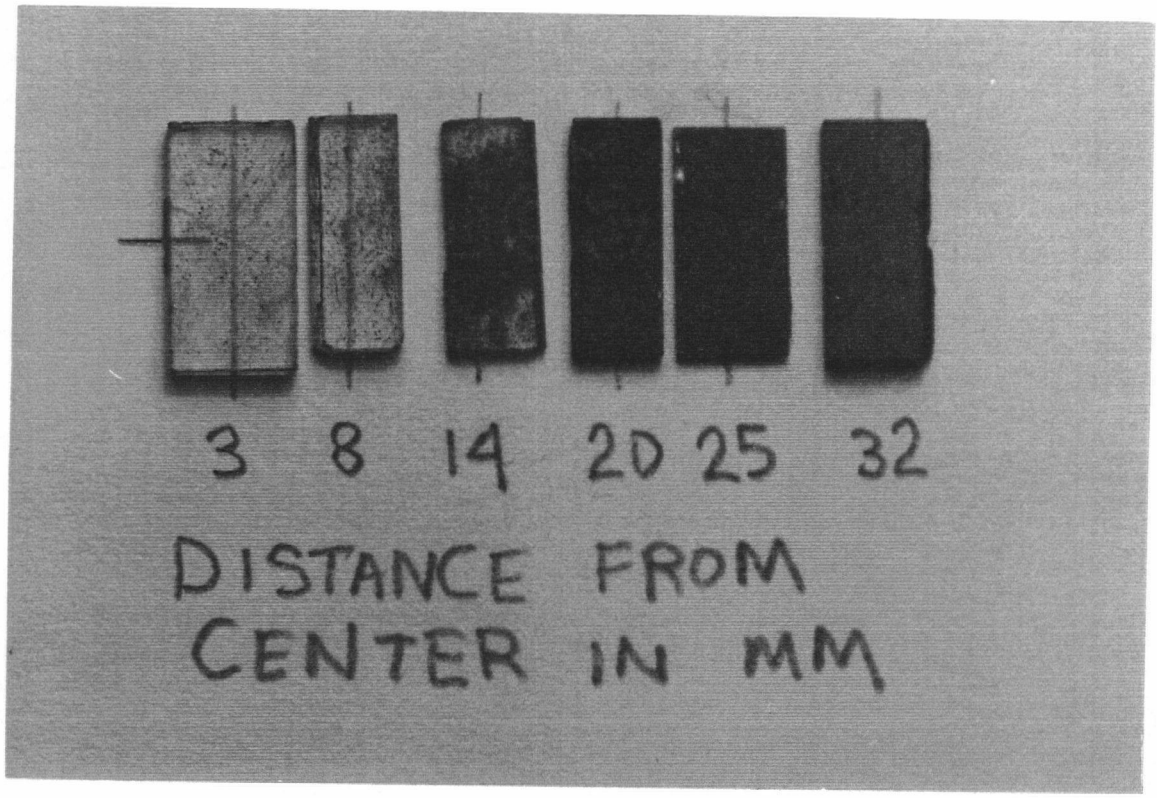

Figure 4.12: Photo of film flaking at different radii during annealing

observation that deviations between the metal and Bi-Sr-Ca-Cu-O film profiles of Figure 4.10 were confined to radii of less than ~2.5 cm — which corresponds to the radius of the target. As well, the darker, opaque film area seen in Figure 4.9 also corresponds to this same region. Finally, films which were deposited in this inner region tended to flake off during the post-deposition processing. (See Figure 4.12 for a photograph of this effect) The boundary between flaked an unflaked film was often very well defined and indicated that adhesion of the film to the substrate underwent a sharp transition at a radius roughly corresponding to that of the target. Clearly, something is affecting the properties of films deposited exactly in the area which is most likely to be affected by negative ion generation at the target.

There are two mechanisms by which such an ion bombardment could have affected

the films in this manner. The first would have been by making the film more dense in the centre (densification) so that as much or more material there took up less volume. The second would have been by simply resputtering a corresponding amount of the film material. How well these two hypotheses account for the results is discussed below.

4.3.1 Densification

A change in submicron structural features such as grain size and orientation (the microstructure) could best explain how the films could become more dense in the centre.

Sputtered film microstructure has been described by Movchan and Demchishin in the Structure Zone Model (SZM).[75,40] The SZM predicts that microstructure will correspond to one of three regimes which are determined largely by the substrate temperature during deposition. Zone 1 growth occurs at the lowest temperatures (substrate temperature less that 30% of the melting temperature) and is characterized by loosely packed columns with void boundaries. Zone 2 growth ($0.3 \leq T_s/T_m \leq 0.5$) consists of more densely packed columns and Zone 3 ($T_s/T_m > 0.5$) has wider, less columnar grains. An intermediate regime subsequently identified by Thornton[40] as Zone T, occurs between Zones 1 and 2, and consists of densely packed but poorly defined fibrous grains. Transitions between zones can be initiated by ion bombardment as well as substrate temperature.

If the microstructure were to change across the Bi-Sr-Ca-Cu-O films, then the density would not be uniform. Films with a greater density in the centre could well have as much or more material than thicker but less dense regions further out. This effect could account for the atypical thickness profile seen in Bi-Sr-Ca-Cu-O films.

This explanation is dependent on a transition between zones occurring across the film. Since the melting temperature of the films is approximately 900°C, the temperature at which one would expect a transition between Zone 1 and a more dense zone such as

Zone T or Zone 2 would be near 80°C. Given the greater expected ion bombardment in the centre of the film, it is plausible that the substrate temperature may have exceeded this in the centre of the film but not at the edges. Thus, an increase in density toward the centre of the film is reasonable given predictions based on the Structure Zone Model. Unfortunately, attempts to directly observe the film microstructure using a scanning electron microscope failed due to inability to resolve any structural detail at the instrument's limit of 0.1μm.

A transition from Zone 1 to Zone 2 (or Zone T) growth in the film directly in front of the target would explain several observations. The profile of the film would be explained by the change in density. The change in opacity would be explained since the inter-columnar voids of Zone 1 growth would transmit much more light than the densely packed Zone 2 (or Zone T) structure. The flaking of the central films during processing could be explained by increased stress due to differential thermal expansion since the higher density provides fewer voids for the film material to expand into.

It should be noted that films deposited onto heated substrates did not flake during processing. However, this may have been because such films would have lower intrinsic stress since the higher surface mobility at elevated temperatures would allow the film to relieve such stress as it grew. Alternatively, the adhesion to the substrate may have been enhanced by the higher temperatures.

The biggest problem with explaining the decline in thickness in the centre of the film by a transition to a more dense film microstructure is the magnitude of the effect. To fully account for the thickness profile, the increase in density in the centre of the film would have to have been by 30% over the values at radii of more than 3 cm. Values obtained by simulation[76] for a Zone 1 to Zone 2 transition indicate an increase in density of only 15%. Therefore, some other mechanism, such as film resputtering, must be invoked to explain the rest of the reduction in film thickness.

4.3.2 Resputtering

As mentioned above, it is also possible that the film was thinner in the centre not because it was more dense, but simply because there was less material there. Given the ion flux that must have been present to cause the substrate bombardment effects observed, some resputtering is probable. The question is to what extent was this factor responsible for the reduced film thickness.

Serious resputtering effects have been observed while sputter depositing the similar Y-Ba-Cu-O superconductors.[77,78] In fact, in an oxygen-rich deposition atmosphere, Rossnagel *et al*[78] were able to resputter the Y-Ba-Cu-O film at a higher rate than they were depositing it. They explain that the bombarding particles were O^- ions produced at the target surface and accelerated away by the negative bias. The ions were stripped of their extra electron by collisions in the plasma and struck the substrate as neutral species. The relevance of this result to the Bi-Sr-Ca-Cu-O system is unknown since the O^- yield of the component species will be different.

The most likely explanation of the Bi-Sr-Ca-Cu-O film properties is that both densification and resputtering were important. The bombardment probably caused microstructural changes which discolored the film and caused stresses which resulted in flaking during annealing. On the other hand, probably half of the thickness reduction was due to resputtering.

The consequence of these effects from an applications point of view is that high quality films cannot be deposited at room temperature in the central zone unless the problem of films flaking is solved. The simplest solution is to only use the material deposited in the annulus from about 2.5 cm to perhaps 4.5 cm; however, this only uses a fraction of the Bi-Sr-Ca-Cu-O material deposited. Alternatively, deposition within the central region seems possible with heated substrates, although this would add to the complexity and

cost of the system.

4.4 Compositional Variations

The growth of the $Bi_2Sr_2Ca_2Cu_3O_y$ phase during processing is reported to be quite sensitive to composition,[62,88] so it is desirable to maintain a high degree of uniformity across as large an area as possible.

Figure 4.11 showed that although the as-deposited films appeared quite uniform across a small area, there was some compositional variation across the entire film — particularly in the copper concentration. This could be explained either by preferential resputtering of the film by the bombarding ions or by an element-dependent ejection angle for sputtered species coming from the target.

Preferred resputtering is a consequence of how well each atom is bonded (chemisorption or physisorption) to the film surface. If the copper is particularly strongly bound, and the other elements are less so, then the copper concentration would be enhanced in the centre by resputtering effects. However, this explanation implies that the region of the film with high copper concentration would be the same as the region with the highest ion bombardment. The above results show the copper concentration dropped off in a region where the ion bombardment was still high.

As it is sputtered, each atom leaves the target surface at some ejection angle to the axis of the deposition. If the distribution of these angles varied with the type of atom or molecule sputtered, then the spatial distribution of each the element would be a different. This could explain the unusual copper distribution across the film.

Since sputtering involves momentum transfer, the obvious variable for determining the distribution of ejection angles would be mass. Unfortunately, this would not explain the Bi-Sr-Ca-Cu-O system where calcium (atomic mass 40) and bismuth (mass 209) had

similar concentration profiles while copper (mass 64) was quite different. Nonetheless, the possibility of some other kind of element-dependence of the ejection angle is supported by observations by Burbidge *et al*[77] with Y-Ba-Cu-O films.

Using optical emission of species in the plasma during dc magnetron sputtering, Burbidge *et al* observed that the relative intensity of yttrium spectral lines decreased away from the axis of the discharge. This decrease was correlated with compositional variations across the film determined by energy dispersive X-ray spectroscopy. Once again, this distribution does not seem to be simply dependent on the mass of the respective elements. A similar optical emission study in the Bi-Sr-Ca-Cu-O system could determine if element dependence of the ejection angle is the source of the compositional variation in the films considered here.

Regardless of the cause of the compositional variations across the films, some measures must be taken to minimize their effects. The easiest solution is to only use an annulus at radii where the composition is relatively uniform. This is reasonable for development work, but inefficient for commercial production. An alternative is to average composition through substrate motion during deposition. The former approach was used in this work.

4.5 Substrate Temperature

A series of studies was conducted to examine the effect of substrate temperature on film properties. There were several motivations for this work. First, Adachi *et al*[29] had reported enhanced production of the 2223 phase on heated substrates. Second, it would be technologically advantageous to be able to produce as-deposited superconducting films which would not require a post-processing step. Obviously, this would require a hot substrate to allow crystallization of the proper phase as the film is grown. Finally, it was suspected that the flaking effects during processing could be relieved by depositing onto

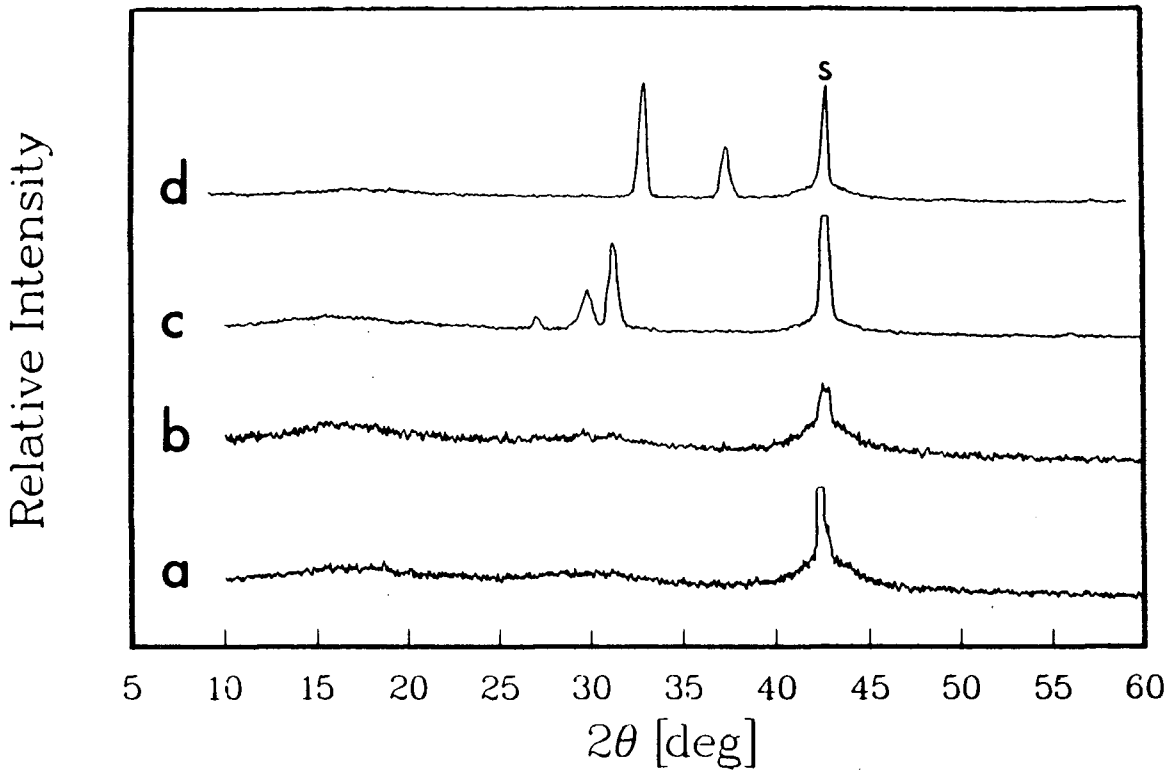

Figure 4.13: X-ray diffraction spectra of films deposited at different temperatures: a) 21°C b) 450°C c) 550°C d) 730°C. 'S' labels the MgO substrate line. The other peaks present are associated with impurity phases. There is no evidence of the growth of the Bi-Sr-Ca-Cu-O superconducting phases.

heated substrates. To examine these possibilities, the effects of substrate temperature during deposition of TB7 (2:2:2:3) films were studied from room temperature to 730°C.

The crystallinity of these films was studied using X-ray diffraction. Figure 4.13 shows the diffraction spectra for several temperatures. These spectra indicate that the films remain amorphous until at least 450°C. Above 500°C, some crystalline peaks begin to form, but they are all due to impurity (non-superconducting) phases. One film deposited at 650°C did have a relatively low room temperature resistance which is often associated with superconductivity, but cooling it in the liquid helium cryostat indicated that it had semiconducting resistance behaviour.

The elemental composition of the films was examined in an effort to determine why the desired phases did not crystallize. The results indicate (See Figure 4.14) that the bismuth

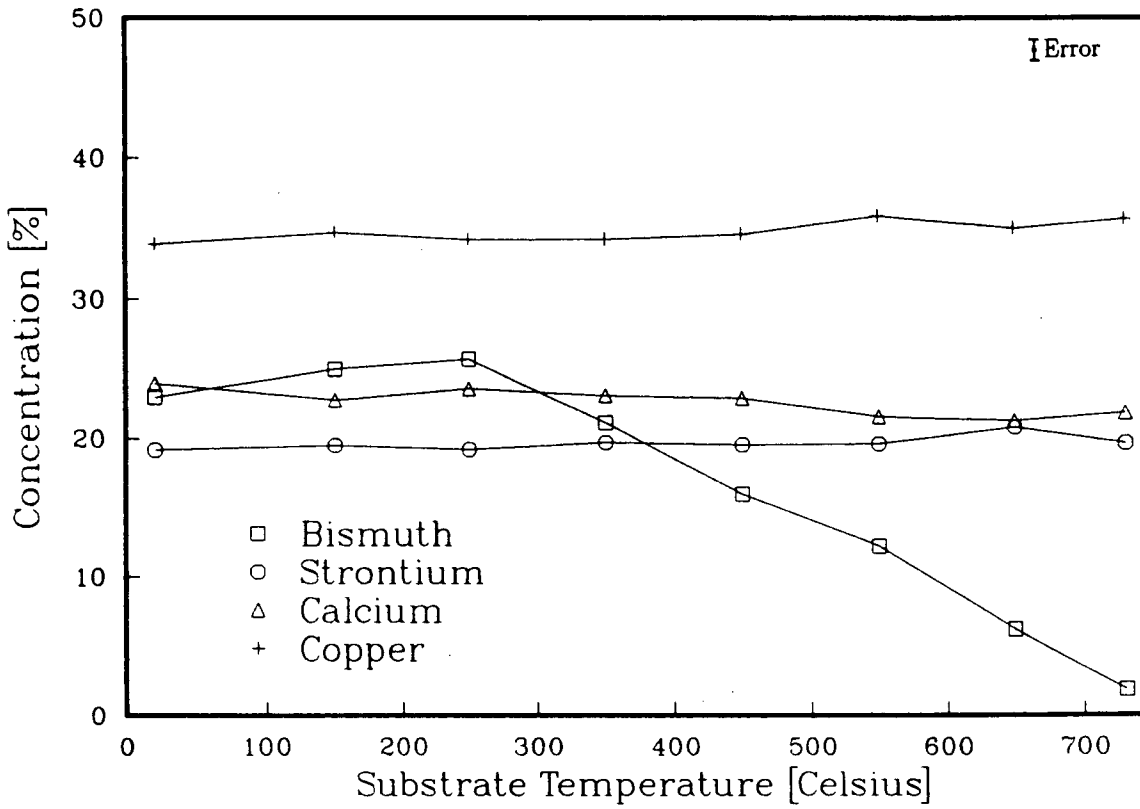

Figure 4.14: Composition of the film as a function of substrate temperature. The values are normalized so that Sr, Ca, and Cu add up to their room temperature total.

concentration in the films dropped off significantly above 350 – 400°C. Consequently, the films with sufficient thermal energy to crystallize lacked the correct stoichiometry. This implies that high quality as-deposited superconducting $Bi_2Sr_2Ca_2Cu_3O_y$ films will not be possible without considerable compensation for the bismuth deficiency.

Film thickness was not seen to diminish significantly with temperature. This indicates that only the bismuth was being lost from the films at a substantial rate. There was no similar drop in the concentration of lead in films made using the lead-doped TB10 target at substrate temperatures up to 500°C.

Several TB5 (4:3:3:4) films deposited near 650°C were processed using the standard conditions described in Chapter 5 for annealing. These films showed a small but definite increase in the amount of the 2223 phase formed over films which were deposited at room

temperature. This effect was even smaller for TB7 (2:2:2:3) films.

4.6 Sputtering Atmosphere

Many of the deposition parameters are dependent on the atmosphere during sputtering. For instance, pressure affects the deposition rate by scattering the sputtered flux and determining the cathode current.[39] Inelastic collisions in the gas also moderate the effects of high energy particles which bombard the substrate. As well, the types of species present in the atmosphere have a strong effect on deposition conditions. Most of the sputtering done in this work involved argon, but impurity gases can influence deposition rates and film purity due to the highly reactive nature of the plasma. Adding reactive gases such as oxygen (see below) can virtually halt deposition and affect the formation of negative ions which bombard the substrate.[39]

It is beyond the scope of this work to consider all of the possible variables that stem from the sputtering atmosphere. Instead, a few basic effects on the deposition of Bi-Sr-Ca-Cu-O films were considered and an effort was made to be consistent in setting the other parameters.

As mentioned above, the sputtering gas used primarily was 0.5 Pa of argon. This was a convenient pressure that allowed both stable discharges and comparatively high deposition rates. Higher pressures such as 1.4 Pa reduced rates by 10-15%, although the effects of ion bombardment were slightly lessened. Pressures much lower than 0.5 Pa resulted in discharges which were difficult to strike and would spontaneously extinguish.

The effect of adding oxygen to the sputtering atmosphere was briefly studied. The motivation for this was the observation that, particularly in the case of $YBa_2Cu_3O_{7-\delta}$, the properties of the high-T_c materials were sensitive to the amount of oxygen present. Since it is relatively easy to introduce oxygen to the system during the processing stage,

this avenue was not pursued beyond the preliminary investigation of effects on deposition properties. The amount of oxygen was increase from 0 to 70%, keeping the total oxygen-argon pressure fixed at 0.5 Pa. Films were sputtered from a 2:2:2:3 target (TB7).

The films were usually transparent yellow and appeared smooth. Profilometry indicated that deposition rate was sharply reduced if the oxygen concentration exceeded 20% (0.1 Pa partial pressure). It is unknown if this reduction was due to the decreased sputtering effectiveness of oxygen with respect to argon, chemical changes at the target surface, or increased bombardment of the substrate by O^- ions. No enhancement of the superconducting properties was observed in these films after processing.

4.7 Target Composition

Table 4.4 lists the operating conditions for all of the targets used. As TB10 was calibrated at 100W, the values in parentheses for this target have been linearly scaled to 80W for comparison with the other targets. As can be seen, the bias voltage and rate varied from target to target — either due to target composition or fabrication. In general, lower bias voltages resulted in higher rates. No other trends are obvious from the data.

Target	Composition (Pb)Bi:Sr:Ca:Cu	Power (±2 W)	Bias (±2 V)	Rate (±1 nm/min)
TB3	2:2:1:2	80	-146	10
TB5	4:3:3:4	80	-152	10
TB7	2:2:2:3	80	-217	7
TB8	4:3:3:5	80	-150	12
TB9	(1)1:2:2:3	80	-233	8
TB10	(2)2:2:2:3	100	-297	15
		(80)	(-238)	(12)

Table 4.4: Sputtering conditions for each target used. All data refer to a sputtering atmosphere of 0.5 Pa of argon. Rates correspond to a radius of 2.5cm.

Chapter 5

Characterization of Processed Films

5.1 Introduction

In order to convert the amorphous as-deposited Bi-Sr-Ca-Cu-O films into crystalline superconductors, an annealing step is required. Complex and interrelated factors govern this aspect of film production. For instance, the processing temperature is highly dependent on initial film composition, the amount of lead dopant in the films, and the atmosphere present during the annealing. Similarly, the duration of the anneal depends on the process temperature, and ramp rates. The composition of the films may vary with the duration of the anneal. Unfortunately, the film properties are highly dependent on all of these factors.

The reaction which forms the $Bi_2Sr_2Ca_2Cu_3O_y$ superconductor is very complex, involving the arrangement of 38 atoms in the unit cell. The understanding of the underlying chemical and physical principles that govern this reaction is still very limited. To determine the best film processing conditions one must consequently rely on empirical results which are complicated by all of the factors mentioned above. A very basic procedure was used here which involved heating the sample at a fixed rate to a fixed temperature for a fixed duration in a particular atmosphere. The goal of this work was to try to identify trends by changing any one of these variables while keeping the others constant. Since all of these factors are interrelated, this approach does not necessarily yield the optimal process, but it does provide systematic information about important variables for film

production.

Another topic dealt with in this chapter is the effects of doping the Bi-Sr-Ca-Cu-O films with lead. The lead had no significant effect on the deposition characteristics or properties of the as-deposited films, but it did influence the annealing conditions and had a major effect on the properties of the processed films. Although this work did not proceed in such a parallel fashion, the effects on processing of the doped and undoped Bi-Sr-Ca-Cu-O films are presented together in the following sections. In this way, the two types of films can be compared and the impact of the addition of lead to the Bi-Sr-Ca-Cu-O system seen most clearly.

The goals of the high temperature processing are to produce films with a high proportion of the 110K (2223) phase, with good surface qualities, high T_c and J_c, and good reproducibility. The impediments to this are usually the domination of the lower-T_c 2212 phase, and the degradation of either the surface or critical temperature.

5.2 Process Temperature and Annealing Atmosphere

The usual approach to increasing the amount of the 2223 phase is to heat the sample to just below its melting point and leave it there for as long as possible.[27,79] This suggests that the ideal processing temperature is closely related to the melting temperature. A problem with this approach was that the melting temperature in these films depended on a variety of factors, such as composition, lead doping, and oxygen pressure during annealing. These factors are discussed below, followed by a study on the dependence of 2223 phase production on processing temperature under a variety of conditions.

The variation of the Bi-Sr-Ca-Cu-O melting temperature with composition can be seen by comparing TB5 films (4:3:3:4) which melted in oxygen near 900°C to TB7 (2:2:2:3) ones which melted closer to 885°C. This variation was confirmed in bulk samples

by Ono *et al*[63] who observed melting temperatures in air ranging from 872°C to 892°C with very slight changes in stoichiometry. The manner in which melting temperature depended on composition seems quite complex. This sensitivity to changes in composition means that uniformity and reproducibility of the films will be important to film quality.

The amount of lead dopant was also important to determining the melting temperature as films from TB10 ((1.3)2:2:2:3) had a melting point 10–15C° lower than ones from TB7 ((0)2:2:2:3). Oota *et al*[80] found using differential thermal analysis of bulk samples that melting temperature in air decreased monotonically from 878°C ((0):2:2:2:3) to 856°C ((0.9):2:2:2:3) with increasing lead content. This makes comparisons between doped and undoped films more difficult since, ideally, they should processed at different temperatures.

The amount of oxygen present in the atmosphere during annealing was also important. In pure oxygen, TB10 films melted at about 880°C, compared to 863°C in air and less than 850°C in an oxygen-argon mix with about 1% oxygen. This is confirmed by work by Endo *et al*[65] which shows a monotonic decrease in melting temperature of bulk 1:1:1:2 samples with oxygen partial pressure. Their data show a drop from about 890°C in 1 atmosphere of oxygen to about 807°C for pure argon.

As can be seen from these results obtained by myself and others, the melting temperature of Bi-Sr-Ca-Cu-O material is very dependent on a number of parameters. Presumably, these factors will also affect the optimum processing temperature. In order to at least determine trends in 2223 production with process temperature, several of these parameters had to be fixed arbitrarily. As a result, two compositions were picked, one containing lead and one without, and only pure oxygen (1 atmosphere) and air were considered for the annealing atmosphere.

A comparison of different process temperatures is given in the following figures. Figure 5.15 shows the resistance behaviour of TB5 (4:3:3:4) films annealed in oxygen

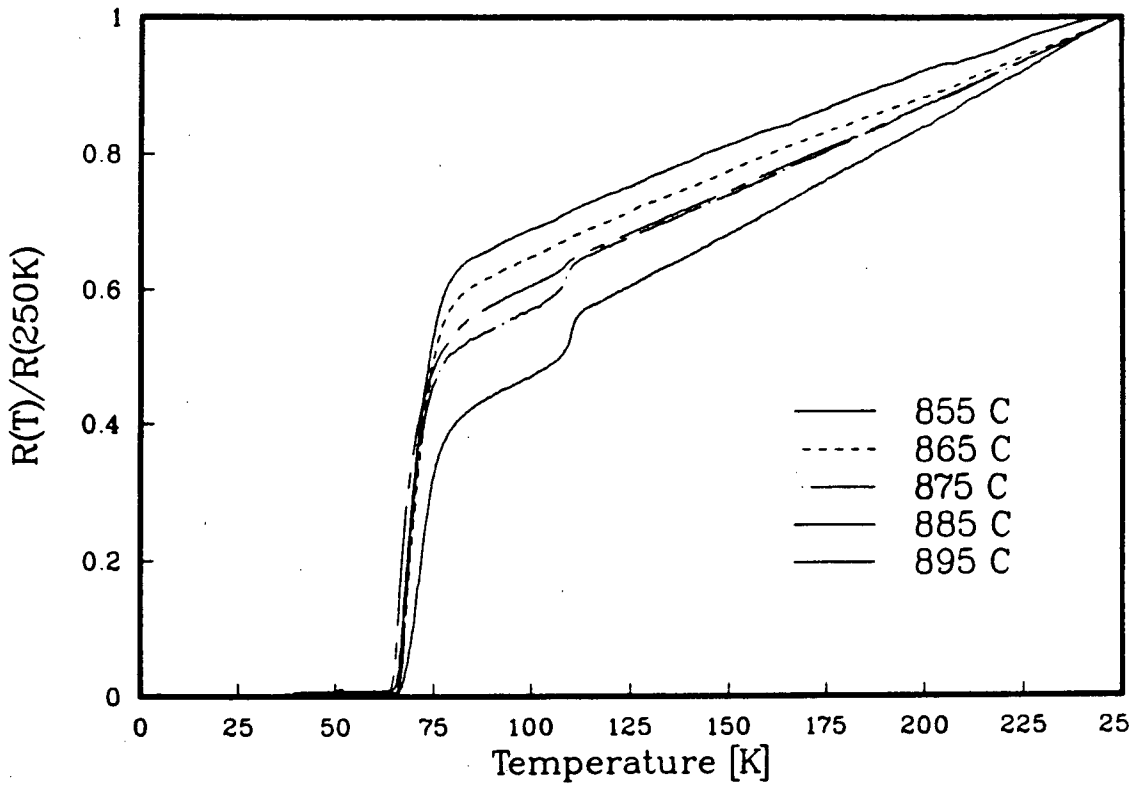

Figure 5.15: Resistance behaviour of TB5 films as a function of annealing temperature in oxygen. Annealing durations are 16 hours with a ramp rate of ±10°C/min. All resistances are normalized to their values at 250K.

at various temperatures. These data indicate that at temperatures below ~870°C the 2212 phase was solely produced, but as the temperature was increased above this, small amounts of the 2223 phase were produced which led to kinks in the resistance curves near 110K. This production of the 2223 phase was only noticeable in the resistance data as there were insufficient amounts of this phase to be distinguishable in the X-ray diffraction spectra. This put an upper bound of about 2% on 2223 concentration. Annealing in air affected these results little — aside from shifting them to lower annealing temperatures.

The situation was quite different with the lead doped films. XRD spectra of such films (TB10 - (1.3)2:2:2:3) annealed in air show a significant amount of the 2223 phase was present. (See indicated curves in Figure 5.17) Judging by the relative intensities of the

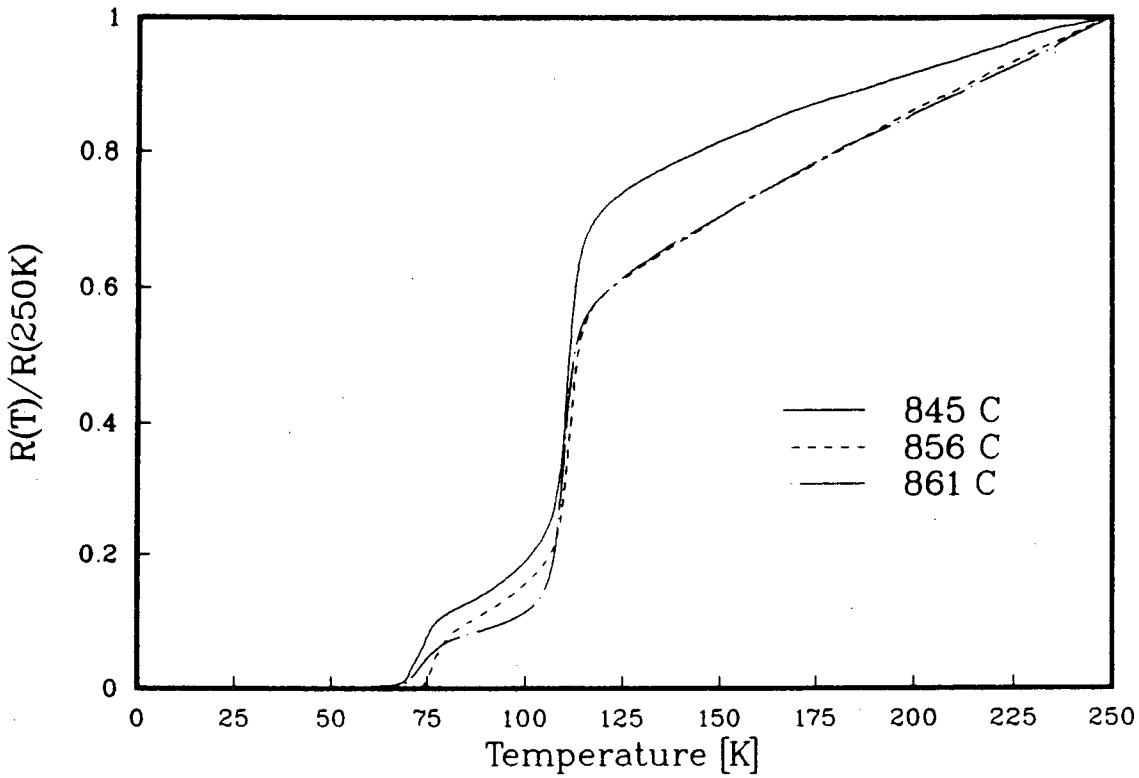

Figure 5.16: Resistance behaviour of TB10 films as a function of annealing temperature in air. Annealing durations are 16 hours with a ramp rate of ±10°C/min. All resistances are normalized to their values at 250K.

2223 and 2212 peaks in these spectra, the optimum process temperature for producing the 2223 phase seemed to be near 845°C. However, the resistance curves for the same films (Figure 5.16) show that these films still had a low T_c due to a poor current percolation path, and the 845°C film actually had the lowest zero resistance temperature of the films considered.

In oxygen, the situation was slightly different for TB10 films. The XRD spectra (See indicated curves in Figure 5.17) show the optimal temperature was near 875°C, although the films started to roughen above 865°C. The resistance data of these films (Figure 5.18) show that the best films were the ones annealed at 865°C which had zero resistance at above 106K. Rocking curves indicated that the superconducting crystals in these films

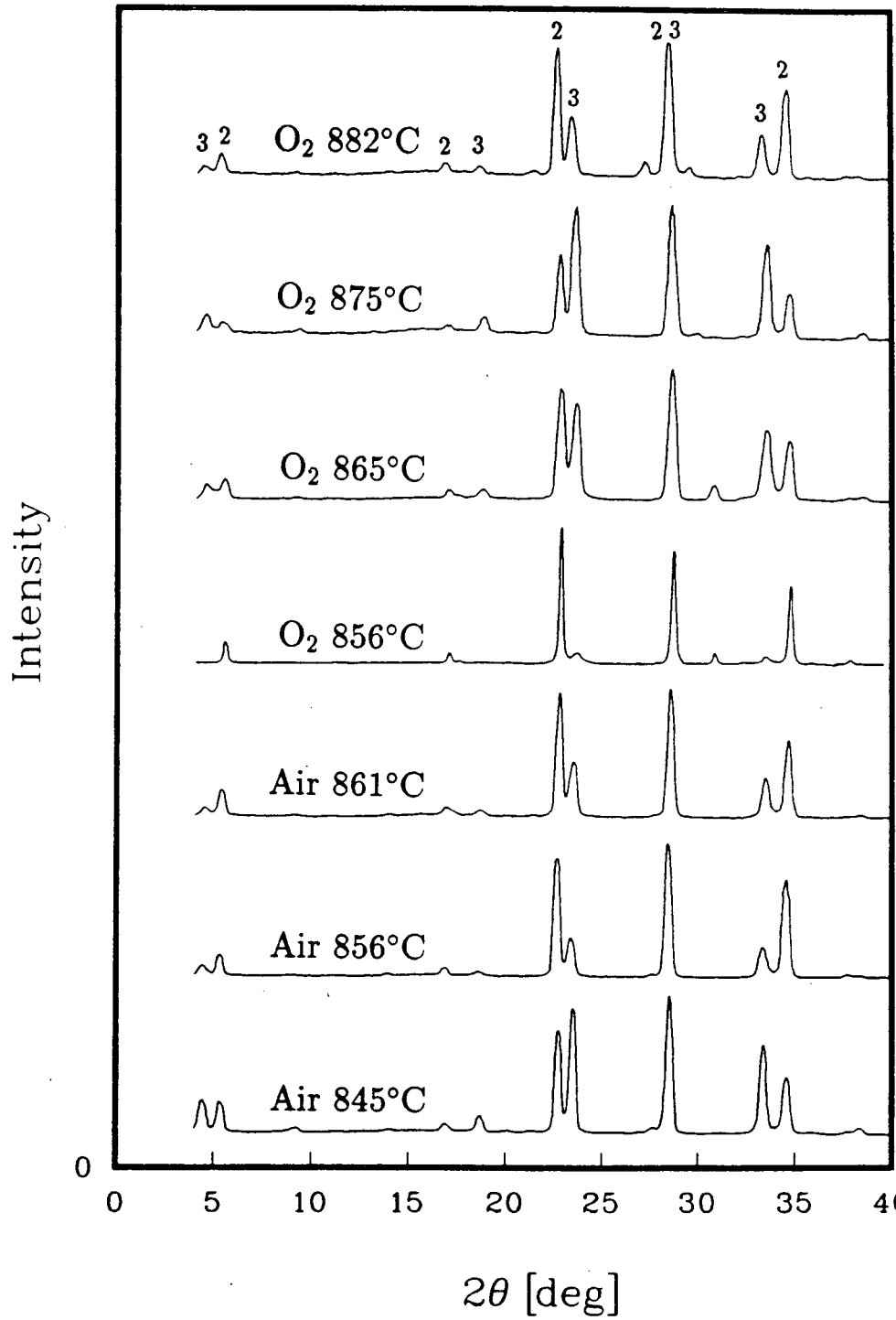

Figure 5.17: X-ray diffraction spectra of TB10 (lead doped) films annealed at various temperatures in air or in oxygen. The duration of all anneals was 16 hours. The (00ℓ) peaks of the 2212 and 2223 phases are labelled by '2' and '3', respectively. Intensities are arbitrary.

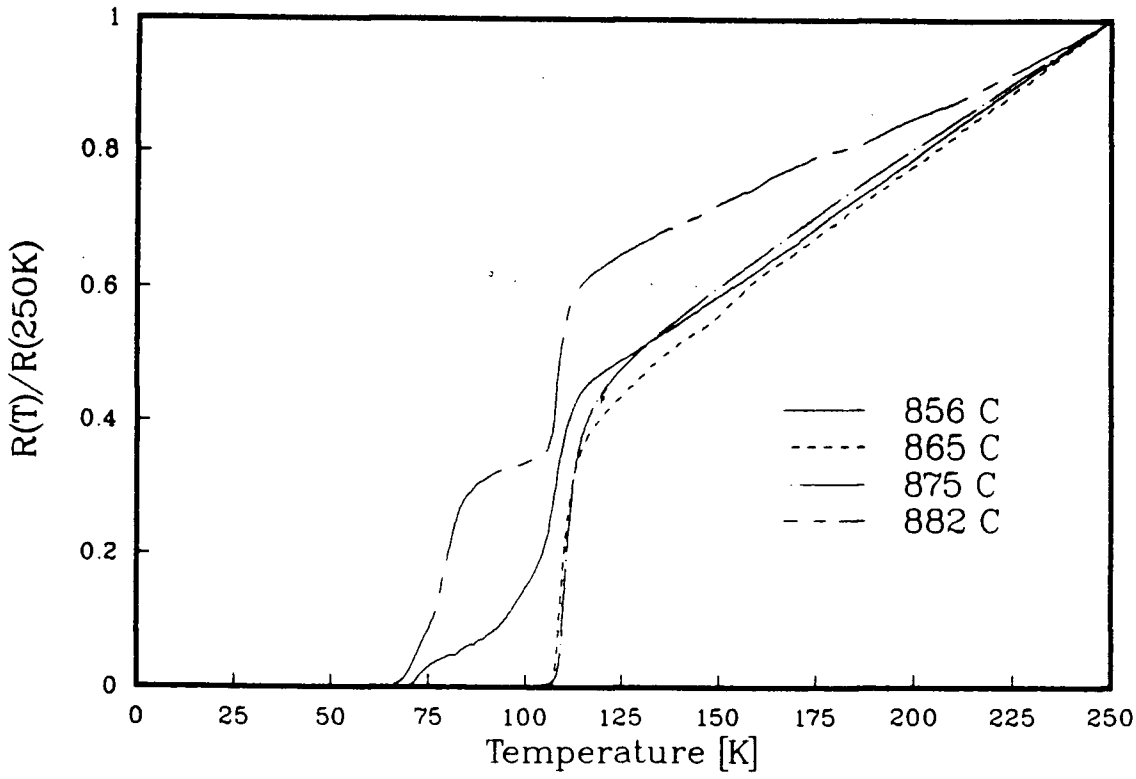

Figure 5.18: Resistance behaviour of TB10 films as a function of annealing temperature in oxygen. Annealing durations are 16 hours with a ramp rate of ±10°C/min. All resistances are normalized to their values at 250K.

were aligned perpendicular to the substrate within ±2° (using ±half width of the peak at half its maximum). Critical currents for these films were on the order of 3000 A/cm^2 at 77K. Both of these last two measurements, however, are subject to the inadequacies discussed in Chapter Three.

Summarizing these results, one can say that only very small amounts of the 2223 phase were produced in the films without lead doping. Furthermore, 2233 was only found in those films annealed near the melting temperature. In lead doped films, significant amounts of 2223 were produced both in air and in oxygen over a much wider temperature range, but the T_c's were lower for films produced in air due to poor electrical percolation. The optimum oxygen annealing temperature for films from TB10 appears to be near

865°C which results in films with T_c's above 100K.

5.3 Duration of Anneal

Fixing the temperature at 865°C and using pure oxygen (the conditions which gave the best results above for lead doped TB10 films), the effects of annealing duration on the development of the 2223 phase were examined in doped and undoped films. This study provided important information about the dynamics of the reactions which form the Bi-Sr-Ca-Cu-O superconductors, as well as information about optimizing the duration of the anneal. In addition, the effect of annealing on film composition was examined.

Two series of films, one from each of TB10 ((1.3)2:2:2:3) and TB7 (2:2:2:3), were annealed for times which varied from 30 seconds to several hours.[81] Films with less than 1 hour of annealing were inserted into and withdrawn from the hot furnace over a period of about 30 seconds (quick cooling). Ramping the temperature from and to room temperature was not practical for these short duration films because the time required to do so is long compared to the time these films were at the process temperature. However, due to the better control afforded by computer controlled ramping, the films with annealing times longer than 1 hour were heated and cooled at the standard ramp rate of ± 10°C/min (slow cooling). All of the films were examined for changes in composition using the electron microprobe and for changes in the crystal structure of the films using the X-ray diffractometer.

5.3.1 Changes in Composition with Annealing Duration

Examination of the films using the microprobe (1 μm diameter beam) indicated that the as-deposited films had very uniform composition, but the annealed films could have considerable variation over a range of microns. The films containing lead which were

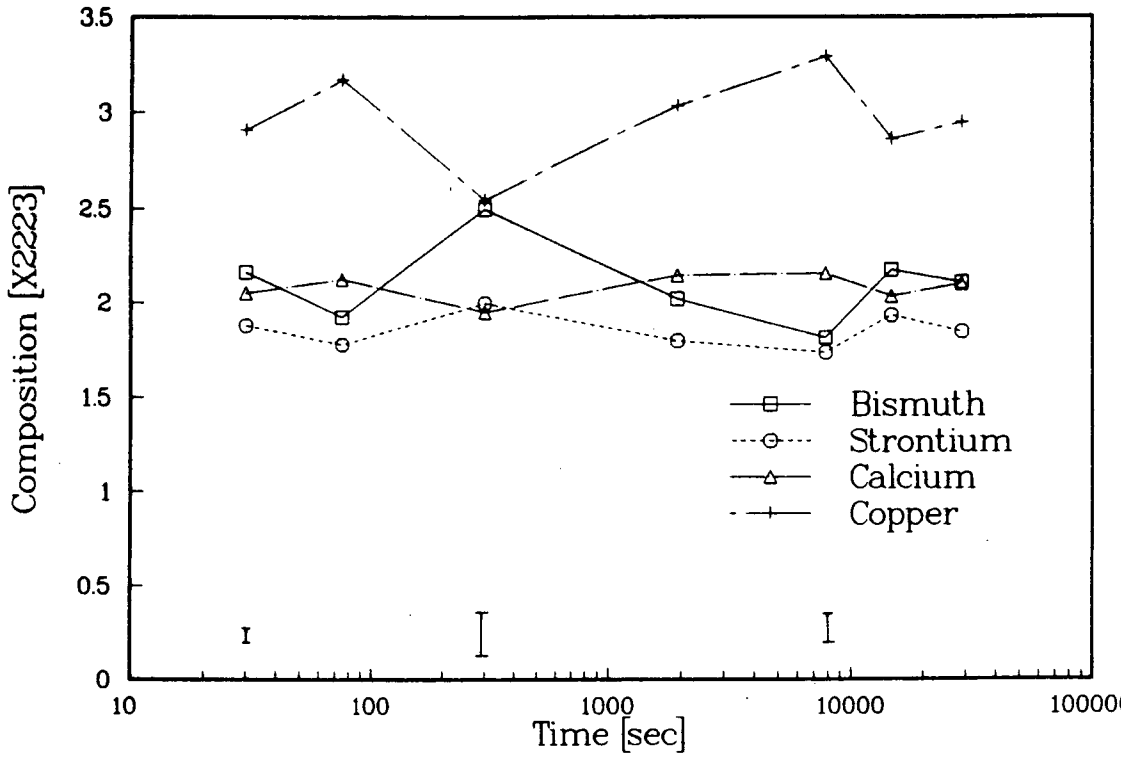

Figure 5.19: Changes in composition of undoped films with annealing. Composition is normalized to Bi+Sr+Ca+Cu = 2+2+2+3. Typical error bars are shown for different times.

annealed for very short times (up to 5 minutes) were still glass-like in appearance and fairly homogeneous. However, intermediate durations of 5 to 30 minutes resulted in light coloured islands with composition (0.5)2.6:2.3:2.0:2.2 forming in the darker background of (2.1)2.0:2.5:3.3:1.2. Times longer than 30 minutes resulted in films which appeared more uniformly black, but which still showed some compositional fluctuations.

Undoped films did not segregate as visibly as the doped films, but appeared more granular and rough. Oblong crystals grew in the undoped films which appeared to correspond to the $(Sr_{0.45}Ca_{0.55})_3Cu_5O_y$ and $(Sr_{0.08}Ca_{0.92})_2CuO_y$ impurities reported by Numata.[64]

Using average compositions, trends in film composition with increasing duration were investigated. There was considerable scatter in the composition of the undoped films

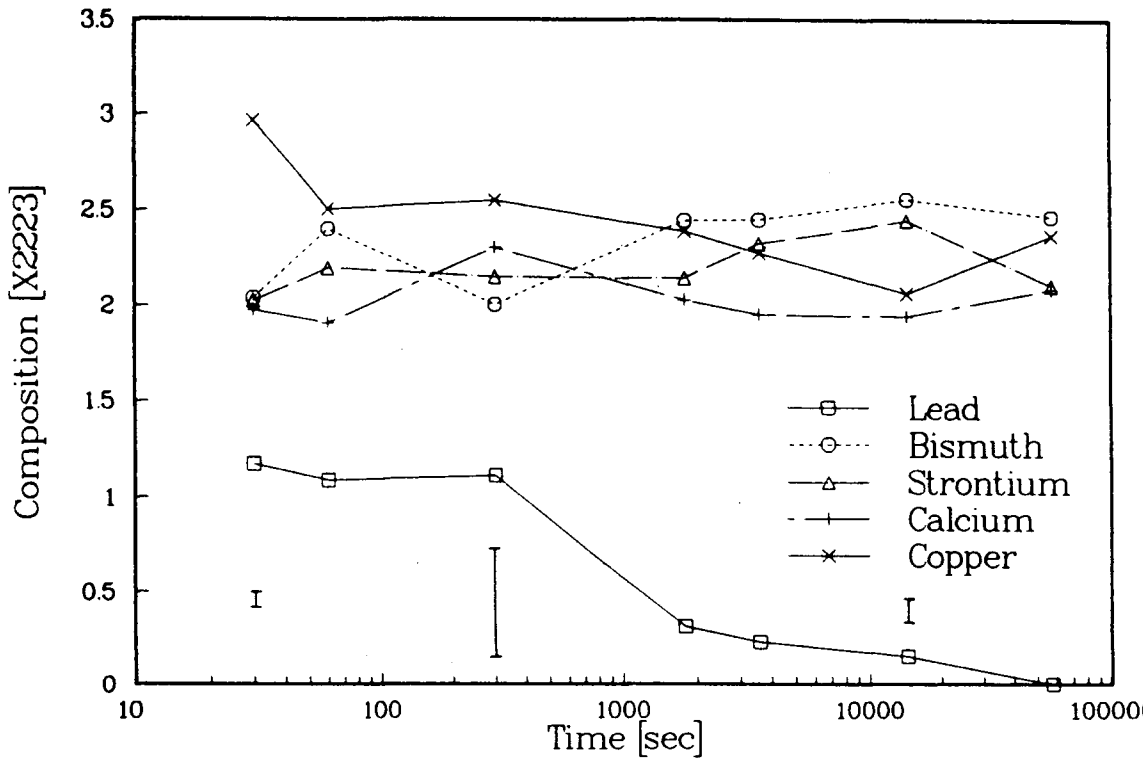

Figure 5.20: Changes in composition of doped films with annealing. Composition is normalized to Bi+Sr+Ca+Cu = 2+2+2+3. Typical error bars are shown for different times.

(See Figure 5.19), but the overall trends show no significant deviations with annealing duration. For the doped films (See Figure 5.20), there was a definite decrease in the relative amount of copper in the films, and a relative increase in bismuth. More dramatic, however, was the sharp decline in the amount of lead. After 16 hours (57600 seconds) of annealing, no detectable amounts of lead remained in the TB10 films tested.

A significant loss in lead has been reported in bulk samples by other researchers,[85, 52,71] but in these cases, the loss of lead was neither so dramatic nor so complete. The quartz furnace tube became slightly discolored downwind of the film during annealing indicating that evaporation is the probable cause of the lead (and copper) losses. Since the exposed surface area-to-volume ratio is higher for a film than a bulk sample, this may

explain why lead losses are apparently more dramatic for films than for bulk material.

5.3.2 Changes in Crystal Structure with Annealing Duration

X-ray diffraction indicates that the films are generally of mixed phase, but the most prominent features correspond to (00ℓ) reflections from the 2201, 2212, and 2223 phases. The XRD spectra of these films were examined for trends with longer annealing.

The films containing lead (See Figure 5.21) developed in three distinct stages. In films annealed for just a few minutes, the 2201 phase was most prominent. For those with about 5 minutes to 1 hour of annealing, the films were almost solely 2212 phase. Finally, for films annealed for more than 1 hour, the 2223 phase started to become significant. The amount of 2223 increased (with respect to the amount of 2212) for the first 8 hours of annealing. Beyond this, no further improvement was seen up to 36 hours (not shown). Given these results, it is reasonable to assume that lead doped films grow in stages which are dominated by first the 2201 phase, then the 2212, and finally the 2223. The 2223 growth halt after about 8 hours corresponded well to the reduction of the amount of lead in the film (as seen in the previous section) to essentially zero.

In the films without lead doping (See Figure 5.22), the situation was somewhat different. These films also had an initial 2201 growth stage, but it did not last for as long. The film annealed for only 1 minute was already predominantly 2212 — although some 2201 was still visible in the 5 minute sample. Films with longer annealing showed increased intensity of the 2212 peaks for the first hour, but the intensity was essentially constant after that. No significant growth of 2223 was seen in the XRD spectra of any of the films even after up to 80 hours of annealing (not shown).

This sequence of $(Pb_x)Bi_2Sr_2Ca_{n-1}Cu_nO_y$ growth in the sequence n=1,2, and then 3 has not been reported elsewhere, but Hatano *et al*[71] and Kim *et al*[82] did report bulk samples shift from initially being predominantly 2212 to increasingly 2223 with

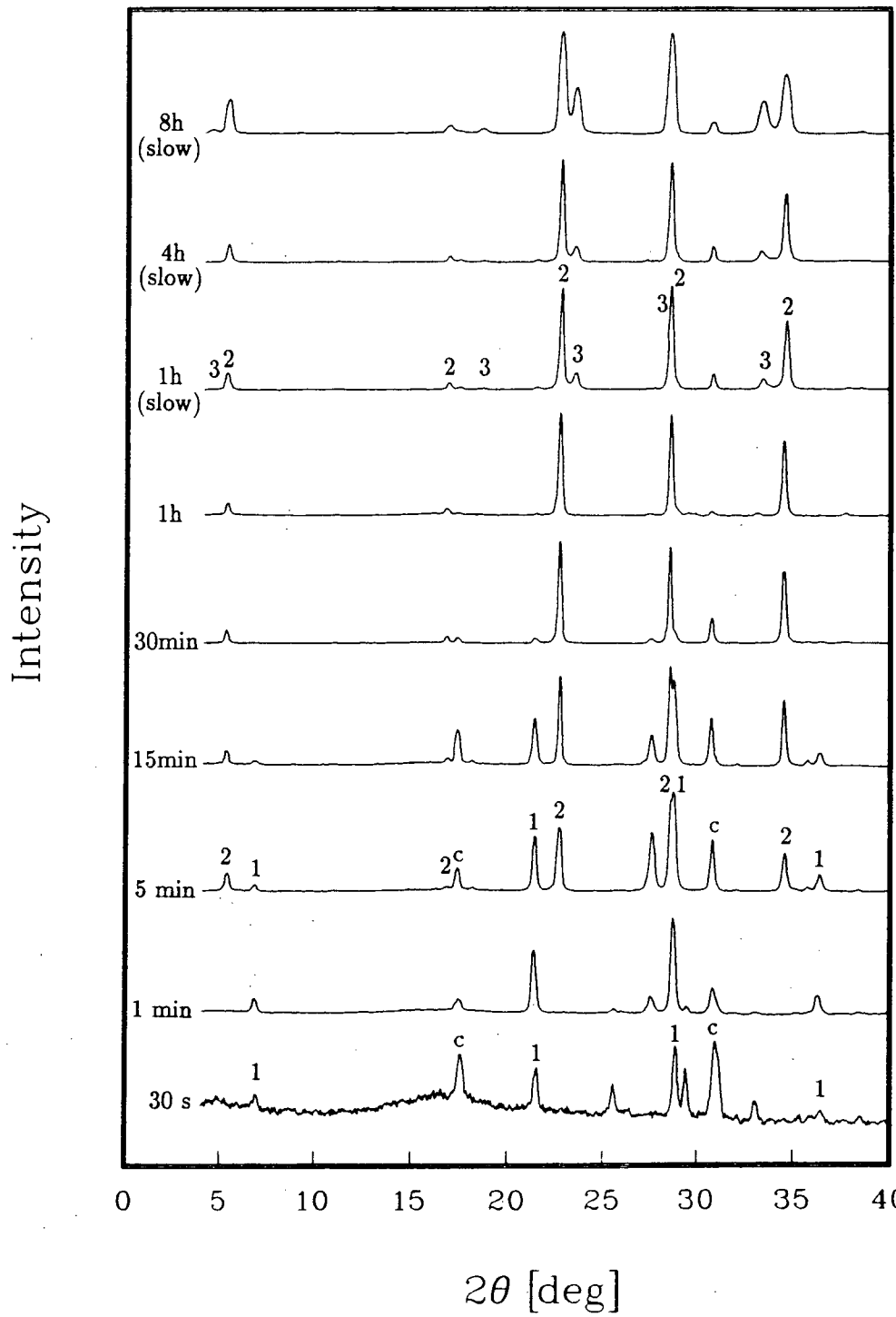

Figure 5.21: X-ray diffraction spectral of lead doped films for various annealing times. 2201, 2212, and 2223 (00ℓ) peaks are labelled '1', '2', and '3', respectively. Ca_2PbO_4 is labelled by 'c'.

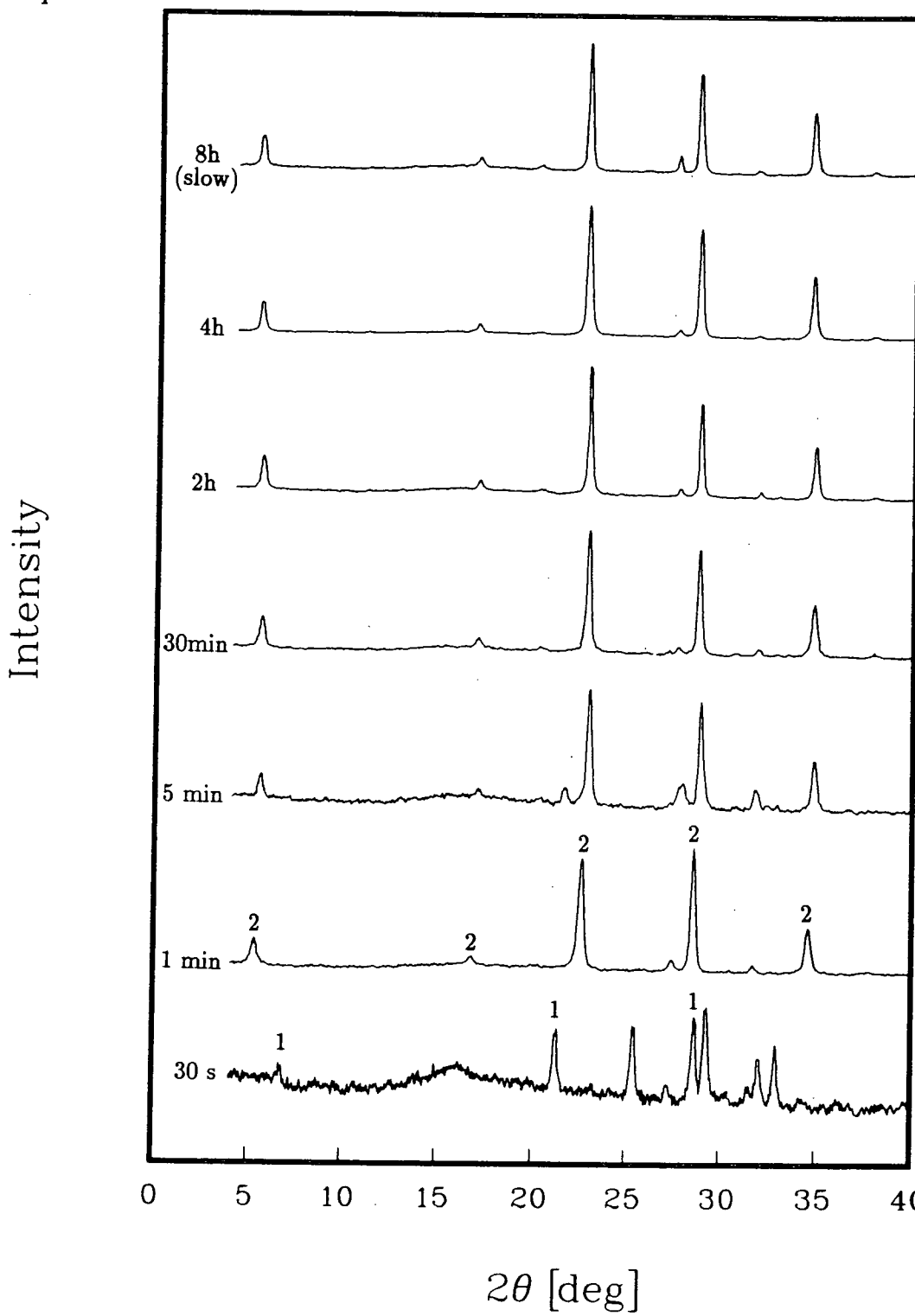

Figure 5.22: X-ray diffraction spectral of undoped films for various annealing times. 2201 and 2212 (00ℓ) peaks are labelled '1' and '2'.

time. However, they observed this conversion happening on a much longer time scale. Also, Hatano *et al* report that the 2201 phase can be present well into the reaction, and that some 2223 starts to form relatively early. Their data does not show the distinct growth through 2201, 2212 and then 2223 stages seen in the films described above. This difference may be due to the less homogeneous starting conditions and slower diffusion in the bulk material.

5.4 Effect of Ramp Rate

In general, ramp rates can be important to film production. Heating and cooling rates can affect the buildup of thermal stresses which contribute to film flaking and cracking. However, in these Bi-Sr-Ca-Cu-O films, the most important effects of ramp rates were to control film properties other than stress.

One would expect that controlling the buildup of stress during film heating is important since, as discussed in Chapter Four, some of these films can flake very readily. However, the deposition conditions seemed to be far more important than ramp rates to determining whether or not a film flaked off of the substrate. Films which were deposited in the central 2.5–3 cm of the discharge generally flaked off during heating even at rates approaching as small as a degree per minute. Films deposited outside of the central zone rarely had flaking problems even with rates of hundreds of degrees per minute.

Similarly, the major role of the cooling rate did not appear to be the control of thermal stress. However, other film properties seem to be strongly affected by the film cooling rate. A TB5 (4:3:3:4) film which was 'quenched' to room temperatures from 882°C over a two second interval showed a much higher room temperature resistance (22 Ω) than a corresponding slowly cooled sample (2-3 Ω). In addition, the slope of the resistance curve above T_c was lower for the quenched film than usual (See Figure 5.23) and the sample

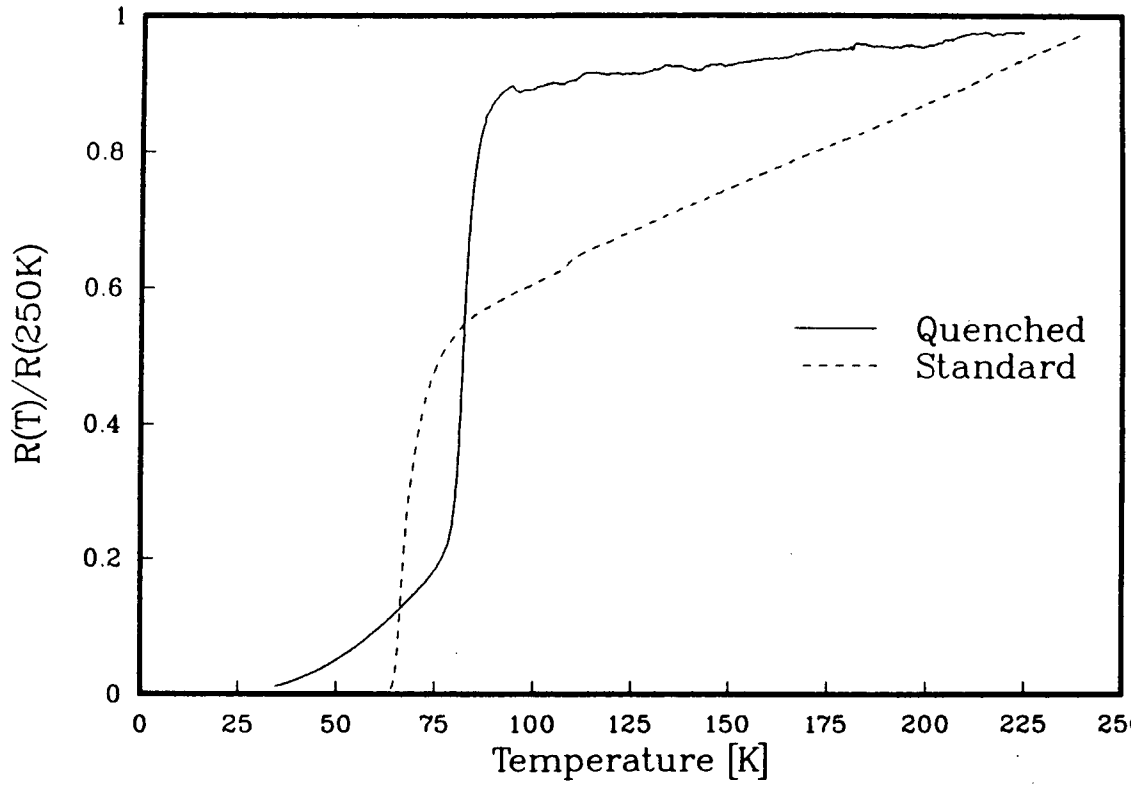

Figure 5.23: Effect of quenching on resistance behaviour of a TB5 sample (annealed at 882°C for 5.4 hours in flowing oxygen). Data for a similar film which was cooled at the standard 10°C/min rate is also shown.

had a depressed T_c. Even though the zero resistance temperature of the quenched film was lower, the bulk of the resistance transition was at a higher temperature and was sharper than for the slowly cooled sample.

There was also a difference in the two lead-doped films which were annealed for one hour in the annealing duration study of Section 5.3. The one which was quickly cooled had a rougher surface and much less of the 2223 phase (determined by X-ray diffraction — See Figure 5.21) than the slowly cooled one. This suggests that cooling rate may be an important factor to 2223 production. Hatano *et al*[71] have also suggested this. The effect of ramp rate on 2223 production is clearly an area where more work is necessary to determine what the important effects and factors are.

5.5 Optimum Lead Doping

Results presented so far in this chapter show that lead enhanced the production of the 2223 phase in Bi-Sr-Ca-Cu-O films. The next step toward optimizing the amount of this phase is to determine how much lead should the films be doped with.

The initial assumption was that lead readily substituted for bismuth. Consequently, a target (TB9) was prepared with composition (0.7)1:2:2:3. However, films from this target consistently contained significant amounts of impurity phases, little 2212 and no 2223. This was presumably due to the large loss of lead during annealing which left a shortage of cations to occupy the (Pb)Bi site. Targets which had a composition based on the assumption that lead substitution for bismuth was negligible were much more successful.

A series of (x)2:2:2:3 films was prepared by sputtering from two targets with different compositions.[83] Ten layers from each of TB7 (2:2:2:3) and TB10 ((1.3)2:2:2:3) were sputtered sequentially to facilitate diffusion of lead throughout the film. Films with lead concentrations of $x = 0.0, 0.26, 0.52, 0.78, 1.04, 1.30$ were produced in this manner. Processing was done at 865°C in flowing oxygen for 36 hours (and also at 8 and 16 hours to confirm these results). These films were characterized by X-ray diffraction (See Figure 5.24) and by determining their low temperature resistance behaviour (See Figure 5.25).

Samples with $x \leq 0.26$ had poor structure and resistance behaviour. Only low intensity 2212 peaks were present in the XRD spectra, and some of these indicated crystal growth that was not oriented with the substrate. Very little 2223 was formed. These films all have long tails in their resistance curves.

For films with $0.52 \leq x \leq 0.78$, well-oriented 2212 peaks were present in their XRD spectra and their resistance transitions were relatively sharp. However, there was still

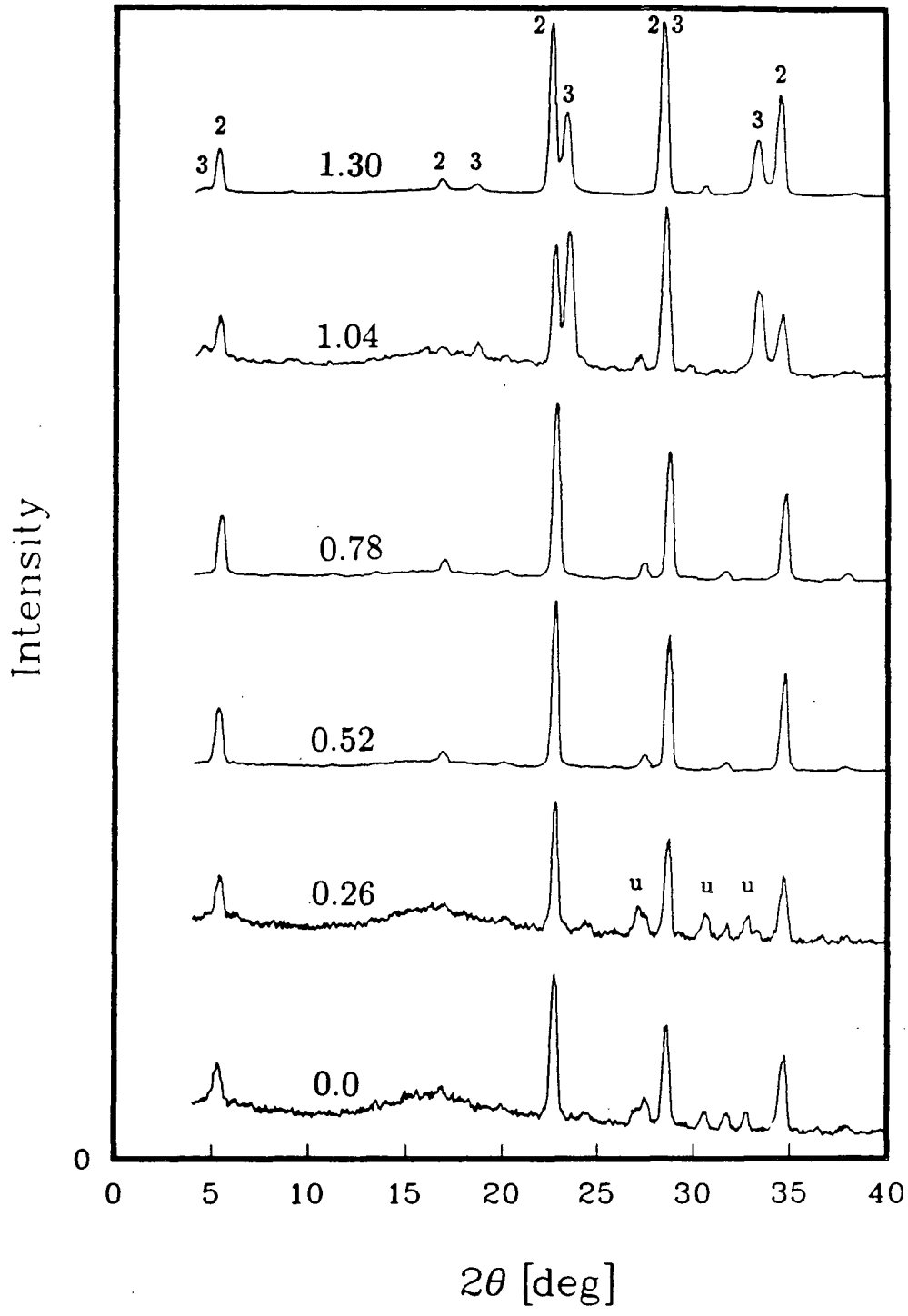

Figure 5.24: X-ray diffraction spectra of films with varying amounts of lead doping. Values given correspond to value of x in the nominal composition $Pb_xBi_2Sr_2Ca_2Cu_3O_y$. Oriented (00ℓ) peaks of the 2212 and 2223 phases are labelled by '2' and '3', respectively. Unoriented (115), (117), and (200) peaks of the 2212 phase are labelled 'u'

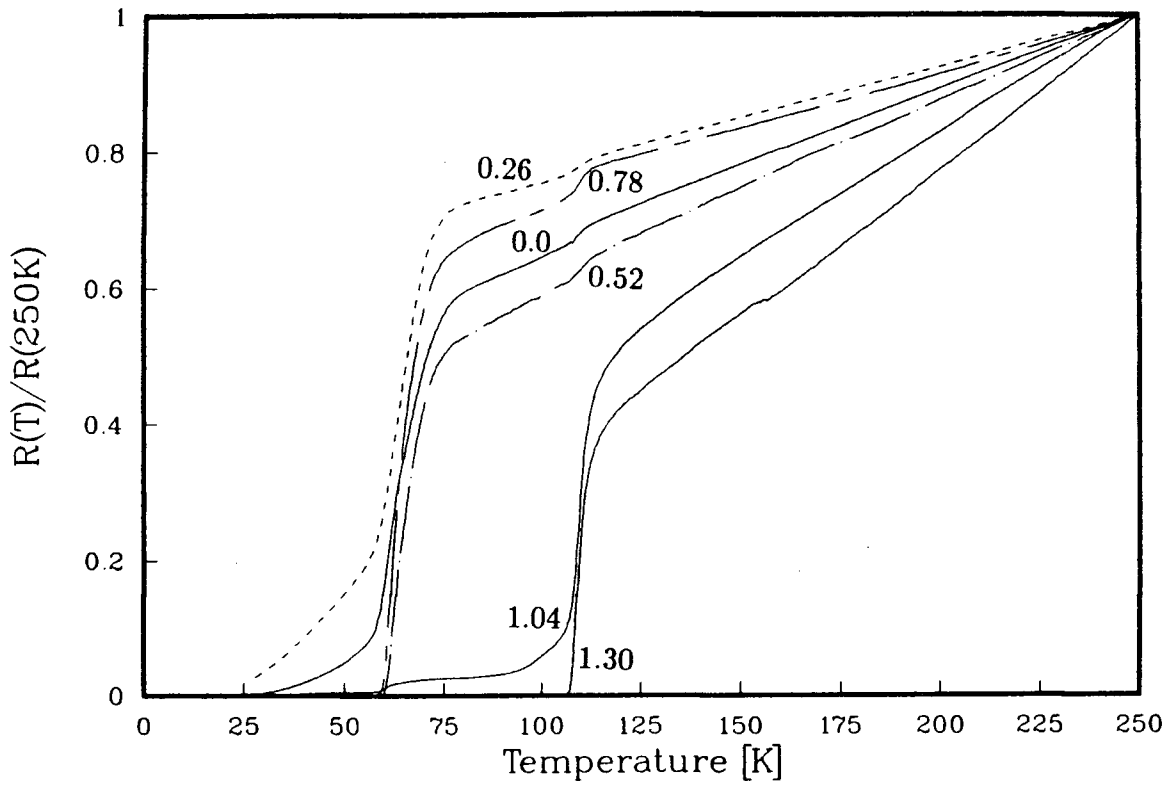

Figure 5.25: Resistance versus temperature for films with varying lead concentration. Resistances are normalized to the value at 250K.

very little 2223 formed. Near x=0.78, the film surface was laced with large needle-like transparent crystals with the approximate composition (determined by microprobe analysis) of $Ca_{.24}Sr_{.16}Cu_{.60}O_?$. These crystals consistently appeared in films with this value of lead doping even under varied annealing conditions.

The samples with x=1.04 had the highest proportion of the 2223 phase in the XRD spectra. However, the absolute spectral peak intensities were quite low and the resistance curve, although having a substantial drop near 110K, had a sizeable tail (Samples annealed for 8 and 16h had much shorter tails). At x=1.30, there was a smaller amount of the 2223 phase visible in the XRD spectra, but the resistance curves show a sharp transition to zero well above 100K. Oota[80] also observed an optimum doping level above which he felt the formation of Ca_2PbO_4 inhibited 2223 formation.

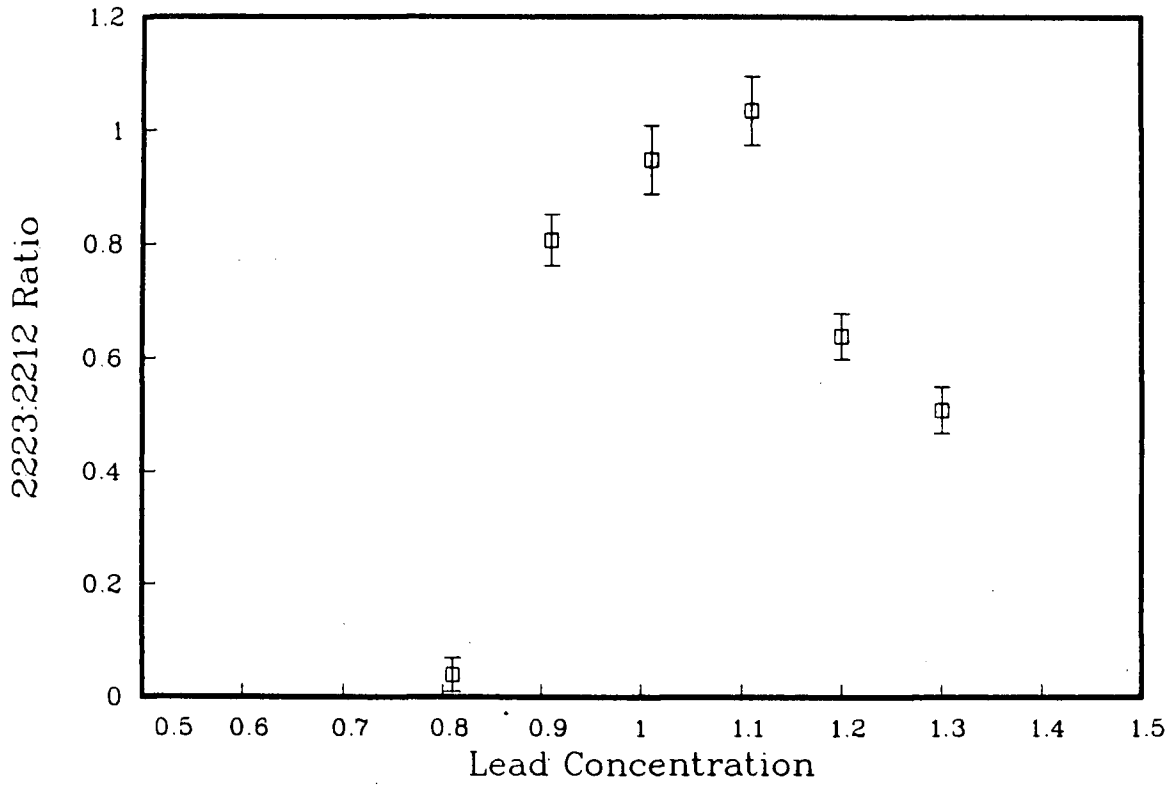

Figure 5.26: Ratio of 2223 (00$\underline{14}$) integrated peak intensities to 2212 (00$\underline{12}$) as a function of lead concentration.

In order to examine the region $0.78 \leq x \leq 1.3$ more closely, six more films were produced with the compositions x=0.81, 0.91, 1.01, 1.11, 1.20, and 1.30. These all showed the presence of 2223 phase (00ℓ) peaks. Figure 5.26 shows the ratio of intensities of the 2223 phase (00$\underline{14}$) peak to the nearby (00$\underline{12}$) peak of the 2212 phase. The data indicate that an optimum value of the lead doping occurs near x=1.1 for the production of the 2223 phase.

The optimum value of 1.1 for the lead composition is above the optimum value of 0.7 determined by Oota[80] for bulk samples (processed at 850°C in air for 170h). This difference is possibly due to a higher rate of lead loss during annealing in films than in bulk material.

5.6 Effect of Lead Doping

This section presents a review of the differences reported above between the lead doped and undoped films and discusses possible mechanisms for explaining how the lead has the effect on 2223 production that it does.

5.6.1 Comparisons between Lead Doped and Undoped Films

There were several major effects caused by adding lead to the Bi-Sr-Ca-Cu-O samples. Most important was the sizeable increase in the production of the 2223 phase under a wide range of conditions. Other effects included a change in the duration of the 2201 stage of development and a possible improvement in surface morphology. The effect on melting and processing temperatures has already been discussed in Section 5.2. This section elaborates on the differences between the doped and undoped films in 2223 production and the 2201 growth stage. As well, a preliminary comparison of the surface structure for the two types of films is given.

Of all of the films produced without lead doping, only two had a significant amount of the 110K phase. The first of these was a severely melted film produced by a complex annealing procedure. Unfortunately, this result could not be reproduced, and the melting of the film had degraded its surface considerably. The second film was also not reproducible and involved extended annealing in air. This film was produced in a furnace previously used to produce thallium superconductors, and it is suspected that thallium contamination was responsible for the enhanced 2223 phase. (Production of Tl-Bi-Sr-Ca-Cu-O superconductors has been reported by others.[6]) In general, large amounts of the 2223 phase could not be reproducibly obtained from undoped films.

Unlike the undoped films, most of the films produced with lead present (TB10) resulted in significant amounts of the 2223 phase. Given an annealing duration of at least

16 hours, a wide range of annealing temperatures in both air and oxygen produced films with this phase. The dominant effect of the lead was to enhance the production of the 2223 phase.

The lead also had some effect on the sequence of film growth. Undoped films had a very short period of 2201 growth before the 2212 phase became dominant. The 2223 phase never started to grow in appreciable amounts. In doped films, the 2201 stage of growth was extended for several minutes, and the 2223 stage started after about 1 h. The extended 2201 stage was well correlated with the amount of Ca_2PbO_4 impurity present in the doped films and may be partly explained by it.[84]

Figure 5.27 shows electron micrographs of the surfaces of films with and without lead doping. The doped film was clearly flatter, smoother, and contained fewer voids. In addition, the long spiked Ca-Sr-Cu-O crystals were absent from the lead doped surface. However, more data needs to be collected to clearly establish a relation between lead content and film surface.

5.6.2 Mechanism For Enhancing 2223 Production

The enhancement of the 2223 phase by lead doping is well established by this work and by others.[66,85,62] What has yet to be determined is the role the lead plays in this enhancement. The two most plausible theories are based on either atomic substitution leading to improved stability of the 2223 phase[86] or on an improved flux mixture for transporting the calcium and copper atoms to their desired sites in the lattice.[87]

Observation of lead directly substituting in the bismuth sites has been reported by a few groups.[86,60] However, this substitution is relatively infrequent, and most of the lead either evaporates or segregates. Nobumasa *et al*[86] report a lead to bismuth substitution ratio of 1:9 based on high resolution electron microscopy.

The results reported in Section 5.3.1, however, showed that some of the best

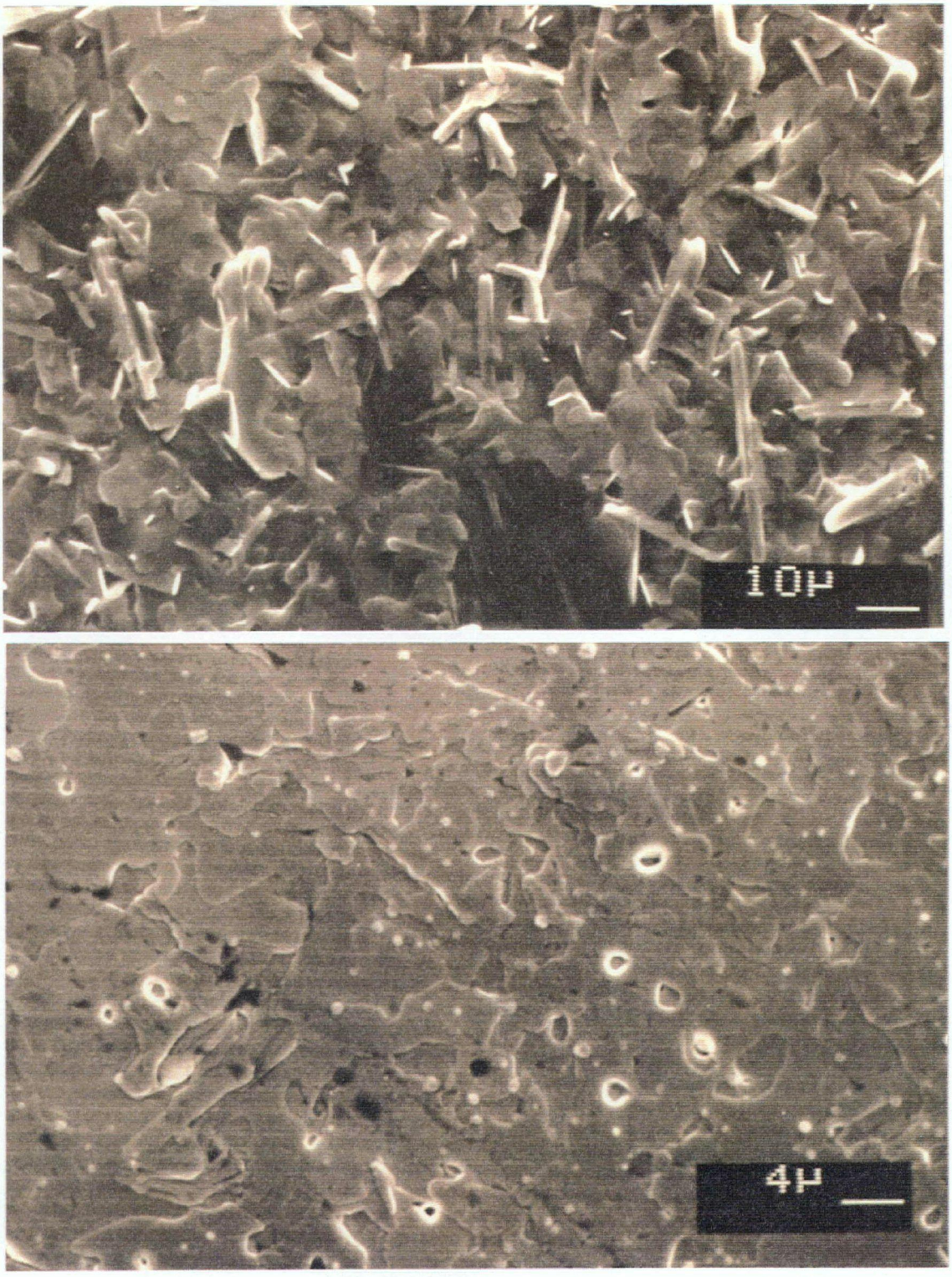

Figure 5.27: Electron micrographs of undoped (top) and doped (bottom) thin films. Note that the scales of the two photos are different.

Bi-Sr-Ca-Cu-O films produced contained no detectable lead at all. Given the sensitivity of the microprobe used, this puts an upper limit of 1–2% for the amount of bismuth which could have been substituted by lead. Yet these films had a substantial (30–50%) amount of the 2223 which was not present in undoped films. This suggests that, while (permanent) lead substitution for bismuth may have been possible, it was not the mechanism by which the lead enhanced the production of the 2223 phase.

The other manner by which the lead can increase the amount of the 110K phase is by forming a more favourable flux for its growth. The flux ideally provides sufficient mobility for the atoms to form the Ca-Cu-O layers that are necessary to progress from 2201 to 2212 and to 2223. The fact that lead lowers the melting point of the Bi-Sr-Ca-Cu-O material means that a region rich in lead could partially melt and form a flux which would enhance the diffusion of the necessary atoms into the desired lattice sites. Partial melting in lead doped samples has been observed by several groups.[71,88,89] Ono[88] also reports that the presence of a small amount of liquid was very important to producing 2223.

In Section 5.3.2 it was observed that the amount of the 2223 phase stabilizes when the lead is essentially completely evaporated. This suggests that the role of the lead is as a catalyst (for example, by producing a more effective flux) rather than as a reactant (such as in a substitution reaction). Otherwise, the amount of 2223 would have decreased as the lead evaporated.

5.7 Methods For Lead Doping

There are several different methods for introducing lead into the Bi-Sr-Ca-Cu-O films. Some experimental work has been done to help determine the best approach for a commercial production setting.

The simplest approach to doping the films would be to mix lead oxides in with the

other constituents when manufacturing the target — as described in Chapter Two. The simplicity and uniform distribution of lead with this approach is a great asset, but the lead loss during target sintering may be difficult to control.

Sputtering metallic lead sequentially with the Bi-Sr-Ca-Cu-O material was also tried. This approach allows greater control over the lead concentration in the films, but it may also require modifications to the annealing process to allow adequate diffusion of the lead throughout the film and to avoid problems with melting the lead. Multilayer deposition with a one hour anneal in oxygen at 300°C (lead metal melts at 327°C[55]) resulted in sufficient diffusion so that the films which were initially reflecting and iridescent due to the lead metal became uniformly transparent. This suggests that a rather minor modification to the annealing procedure is sufficient to allow the lead to diffuse throughout the film when the dopant and film are deposited in layers in this manner.

Since lead is continually lost during the annealing process, however, it may be preferable to introduce the dopant during the processing step. Lead readily evaporates out of the film, but it may be possible to replenish it by placing a source of lead or lead oxide vapour nearby. An equilibrium could be established which would allow one to maintain lead in the film indefinitely to complete the formation of the 2223 phase. The dopant level in the film would be controlled by the partial pressure of the lead-bearing vapour. Such a solution would be especially suitable for thin films which have a high ratio of exposed surface area-to-volume. This high ratio allows volatile materials such as lead to diffuse in (and out) more readily. The main problems with this scheme are the added complexity to the annealing apparatus, and the amount of effort required to determine and control the optimum lead vapour pressures.

The feasibility of supplying lead to the film in this manner has been demonstrated. A silver lined MgO boat containing approximately 1g of PbO was placed next to the film. After a standard anneal, so much lead had been delivered to the film that it had

completely melted and flowed off the substrate or evaporated as a result of the lowered melting temperature.

Supplying or supplementing lead during the processing stage has an important advantage over simply having a fixed initial amount of doping which will slowly be lost during the annealing. In the former approach one can presumably extend the reaction until the 2223 formation is complete (providing the stoichiometry is correct). In the latter case, there is an optimum initial lead concentration (Section 5.5) above which the lead becomes detrimental to producing 2223. The reaction stops when the lead is lost, and conditions must be found to fully form the 2223 phase before this happens. It may be difficult to find such processing conditions given the complexity of the reaction involved.

In summary, adding lead to the target is the simplest approach to doping the films while depositing the lead separately provides greater control over dopant concentration. However, replenishing the system with lead-bearing vapour during the annealing step is likely to be the most effective at producing high purity 2223 films. The feasibility of all three approaches have been verified experimentally.

Chapter 6

Conclusions and Recommendations for Further Work

6.1 Conclusions

The main objectives of this thesis have been met. I have reproducibly made films with large amounts of the $Bi_2Sr_2Ca_2Cu_3O_y$ superconductor and zero resistance critical temperatures of 106K. These films have been characterized and, with a few restrictions, are suitable for prototype development of high-T_c superconductor applications. The procedure I used to fabricate these films was a two step process involving rf magnetron sputtering of an oxide target followed by annealing in oxygen. The effects of many of the production parameters on the quality of the $Bi_2Sr_2Ca_2Cu_3O_y$ films have been investigated and optimized. Both parts of this procedure can be scaled to commercial systems for the production of devices.

In the past year, there has been considerable interest in producing $Bi_2Sr_2Ca_2Cu_3O_y$ films with T_c greater than 100K, but so far few groups have reported making films of high quality. These have been produced through spray pyrolysis[35,90], evaporation[91,92], and sputtering[53,72,93]. While a detailed comparison has not been possible, the films I have produced seem competitive in terms of T_c, reproducibility, and surface quality. Setsune *et al*[53] have reported much higher critical current densities than I have measured, but I feel that my values are understated due to the poor surface of my substrates. Most of my results are as good or better than those reported in the literature.

I have observed several depositional and processing effects not reported elsewhere.

These include ion bombardment of the film during sputter deposition which affected the film profile and caused flaking during annealing. This thesis also describes the first systematic study relating bismuth deficiency with substrate temperature during deposition. The development of Bi-Sr-Ca-Cu-O films through the 2201, 2212, and 2223 stages during the high temperature treatment has not been reported previously. The essentially complete loss of lead in doped films is also novel and gives important information about the role of lead in enhancing the 2223 phase.

In summary, this thesis matter helps to form the ground work for commercial application of $Bi_2Sr_2Ca_2Cu_3O_y$ superconducting films by developing a reproducible production procedure and by characterizing many of the effects that the process variables have on the $Bi_2Sr_2Ca_2Cu_3O_y$ films.

6.2 Recommendations for Further Work

6.2.1 Improvements in Deposition

Two major problems remain with the current method of depositing films. These are the ion bombardment which causes flaking during annealing, and the variation of copper concentration across the film. Currently, these problems limit the fraction of deposited material which is usable film. It would be desirable to use the Bi-Sr-Ca-Cu-O material more efficiently and to produce more films at the same time.

A possible solution to the above problems is to use a moving substrate holder which averages the film composition and bombardment over a larger area. This will certainly reduce compositional variations and allow one to determine an optimum target stoichiometry for producing the 2223 phase. Hopefully, this would also decrease the ion bombardment density sufficiently to prevent the flaking problems. If not, then the problem can probably be alleviated by increasing the sputtering pressure and substrate temperature.

Clearly, an improvement in substrate material is needed. The current MgO crystals used are rough, soft, and expensive. This both limits performance (reduces J_c) of the films and makes them less suitable for applications. An effort to find more suitable substrate materials should be made.

6.2.2 Improvements in Processing

There is little doubt that a better annealing procedure is possible. For example, a single process temperature is unlikely to be optimal for a system which goes through three distinct growth phases. Also, the changing lead level throughout the anneal may require constant temperature compensation. Varying the oxygen pressure during the anneal may be desirable as well, and the effect of cooling rate on the $Bi_2Sr_2Ca_2Cu_3O_y$ films has not been adequately addressed. A study to examine these difficulties will be very challenging, however, and will probably require *in situ* monitoring of the reaction through, for example, X-ray diffraction or differential thermal analysis.

A study could also be made to determine the important parameters for controlling surface smoothness, continuity, and interfacial compound formation.

6.2.3 Improvements in Doping

Of the lead doping methods discussed in Section 5.7, the introduction of lead vapour during processing has the most promise and should be investigated further. Additional dopants could be considered, however, and some success has been reported using antimony[67], praseodymium[68], and barium[69].

6.2.4 Applications

A driving force for this work is the idea that thin films of $Bi_2Sr_2Ca_2Cu_3O_y$ will be useful for device applications. Before this can happen, certain technologies must be developed to make the films more useful. For example, patterning the films, forming diffusion barriers, and attaching leads may be necessary for electronics applications. While developing these techniques is outside of the scope of this work, it is a logical next step in the process of developing applications for high temperature superconducting films.

6.3 Summary

This thesis has discussed many of the important considerations in forming superconducting $Bi_2Sr_2Ca_2Cu_3O_y$ thin films. A simple optimized process for making reproducible high quality samples has been developed which lends itself to further research towards applying high temperature superconductivity.

Bibliography

[1] N.W. Ashcroft, N.D. Mermin, Solid State Physics, Holt, Rinehart and Winston, Philadelphia, 1976, pp. 725–755.

[2] C. Kittel, Introduction to Solid State Physics, John Wiley & Sons, USA, Fifth Edition, 1976, pp. 355–399.

[3] J. Bardeen, L.N. Cooper, J.R. Schrieffer, Phys. Rev. **106**, 162, (1957), **108**, 1175, (1957).

[4] K.A. Muller, J.G. Bednorz, Science, Vol. 237, 1133, (1988).

[5] A.M. Wolsky, R.F. Giese, E.J. Daniels, Scientific American, **260**(2), 60, (1989).

[6] A.W. Sleight, Science, Vol. 242, 1522, (1988).

[7] J. Bednorz, A. Muller, Z. Phys., **B64**, 189 (1986).

[8] C.W. Chu, P.H. Hor, R.L. Meng, L. Gao, Z.T. Huang, Y.K. Wang, Phys. Rev. Lett. **58**, 405, (1987).

[9] A.F. Marshall, R.W. Barton, K. Char, A. Kapitulnik, B. Oh, R.H. Hammond, Phys. Rev. **B37**(16), 9353, (1988).

[10] C. Michel, M. Hervieu, M.M. Borel, A. Grandin, F. Deslandes, J. Provost, B. Raveau, Z. Phys. **B68**, 412, (1987).

[11] H. Maeda, Y. Tanaka, M. Fukutomi, T. Asano, Jpn. J. Appl. Phys. **27**(2), L209, (1988).

[12] Z.Z. Sheng, A.M. Hermann, Nature, **332**, 58–59, 138–139 (1988).

[13] R.J. Cava, B. Batlogg, J.J. Krajewski, R.C. Farrow, L.W. Rupp,Jr., A.E. White, K.T. Short, W.F. Peck,Jr., T.Y. Kometani, Nature, **332**, 814, (1988).

[14] R.J. Cava, B. Batlogg, J.J. Krajewski, L.W. Rupp, L.F Schneemeyer, T. Siegrist, R.B. vanDover, P. Marsh, W.F. Peck,Jr., P.K. Gallagher, S.H. Glarum, J.H. Marshall, R.C. Farrow, J.V. Waszczak, R. Hull, P. Trevor, Nature, **336**(17), 211, (1988).

[15] P. Chaudhari, R.H. Koch, R.B. Laibowitz, T.R. McGuire, R.J Gambino, Phys. Rev. Lett. **58**(25), 2684, (1987).

[16] K. Kuroda, M. Mukaida, M. Yamamoto, S. Miyazawa, Jpn. J. Appl. Phys. **27**(4), L625, (1988).

[17] M.D. Kirk, C.B. Eom, B. Oh, S.R. Spielman, M.R. Beasley, A. Kapitulnik, T.H. Geballe, C.R. Quate, Appl. Phys. Lett. **52**(24), 2071, (1988).

[18] C.E. Rice, A.F.J. Levi, R.M Fleming, P. Marsh, K.W. Baldwin, M. Anzlowar, A.E. White, K.T. Short, S. Nakahara, H.L. Stormer, Appl. Phys. Lett. **52**(21), 1828, (1988).

[19] T. Satoh, T. Yoshitake, Y. Kubo, H. Igarashi, Appl. Phys. Lett. **53**(13), 1213, (1988).

[20] D.J. Mikalsen, R.A. Roy, D.S. Yee, S.A. Shivashankar, J.J. Cuomo, J. Mater. Res. **3**(4), 613, (1988).

[21] C.R. Guarnieri, R.A. Roy, K.L. Saenger, S.A. Shivashankar, D.S. Yee, J.J. Cuomo, Appl. Phys. Lett. **53**(6), 532, (1988).

[22] M. Kanai, T. Kawai, M. Kawai, S. Kawai, Jpn. J. Appl. Phys. **27**(7), L1293, (1988).

[23] T. Venkatesan, X.D. Wu, A. Inam, Y. Jeon, M. Croft, E.W. Chase, C.C. Chang, J.B. Wachtman, R.W. Odom, F. Radicati di Brozolo, C.A. Magee, Appl. Phys. Lett. **53**(15), 1431, (1988).

[24] R.D. Lorentz, J.H. Sexton, Appl. Phys. Lett. **53**(17), 1654, (1988).

[25] J.L. Makous, L. Maritato, C.M. Falco, J.P Cronin, G.P Rajendran, E.V. Uhlmann, D.R. Uhlmann, Appl. Phys. Lett. **51**(25), 2164, (1987).

[26] B. Dam, H.A.M. van Hal, C. Langereis, Europhysics Letters, **5**(5), 455, (1988).

[27] B.T. Sullivan, N.R. Osborne, W.N. Hardy, J.F. Carolan, B.X. Yang, P.J. Michael, R.R. Parsons, Appl. Phys. Lett. **52**(23), 1992 (1988).

[28] M. Hong, J.J. Yeh, J. Kwo, R.J. Felder, A. Miller, K. Nassau, D.D. Bacon, AIP Conf. Proc. No. 182, AVS Series 6, (1989).

[29] H. Adachi, Y. Ichikawa, K. Setsune, S. Hatta, K. Hirochi, K. Wasa, Jpn. J. Appl. Phys. **27**(4), L643, (1988).

[30] H. Yamane, H. Kurosawa, T. Hirai, H. Iwasaki, N. Kobayashi, Y. Muto, Jpn. J. Appl. Phys. **27**(8), L1495, (1988).

[31] A. Asthana, P.D. Han, D.A. Payne, G.C. Hilton, D.J. Van Harlingen, Appl. Phys. Lett. **53**(9), 799, (1988).

[32] D.B. Chrisey, B.P Summers, W.G. Maisch, E.A. Burke, W.T. Elam, H. Herman, J.P. Kirkland, R.A. Neiser, Appl. Phys. Lett. **53**(11), 1001, (1988).

[33] R.S. Liu, Y.T. Huang, P.T. Wu, J.J. Chu, J. Appl. Phys. **27**(8), L1470, (1988).

[34] A. Gupta, G. Koren, E.A. Geiss, N.R. Moore, E.J.M. O'Sullivan, E.I. Cooper, Appl. Phys. Lett. **52**(2), 163, (1988).

[35] H. Nobumasa, K. Shimizu, Y. Kitano, T. Kawai, Jpn. J. Appl. Phys. **27**(9), L1669, (1988).

[36] Y. Akamatsu, M. Tatsumisago, N. Tohge, S. Tsuboi, T. Minami, Jpn. J. Appl. Phys. **27**(9), L1696, (1988).

[37] P. Prieto, G. Zorn, R. R. Arons, S. Thierfeldt, M.E. Gomez, B. Kabius, W. Sybertz, K. Urban, Solid State Comm., **69**(3), 235, (1989).

[38] L.J. Maissel, R. Glang, Handbook of Thin Film Technology, McGraw-Hill, Toronto, 1970.

[39] J.L. Vossen, W. Kern, Thin Film Processes, Academic Press, New York, 1978.

[40] R.F. Bunshah, Deposition Technologies for Films and Coatings, Noyes Publ., New Jersey, 1982.

[41] F.F. Chen, Introduction to Plasma Physics and Controlled Fusion, Plenum Press, New York, Second Edition, 1984.

[42] A.I. Golovashkin, Sov. Phys. Usp. **30**(8), 659, (1987).

[43] D. Caplin, Nature, 335, 204, (1988).

[44] B. VanDover, Lecture at American Vacuum Society 35 National Symposium, Atlanta, Oct. 4, 1988.

[45] T. Yoshitake, T. Satoh, Y. Kubo, T. Manako, H. Igarahi, Jpn. J. Appl. Phys, **27**(6), L1094, (1988).

[46] T. Hidaka, M. Oda, M. Suzuki, Y. Maeda, Y. Enomoto, T. Murakami, Jpn. J. Appl. Phys, **27**(4), L538, (1988).

[47] M. Klee, G.M. Stollman, S. Stotz, J.W.C. deVries, Solid State Commun. **67**(4), 613, (1988).

[48] H. Zhang, S. Yan, W. Zhang, Z. Shen, Y. Sun, G. Li, K. Wu, Solid State Comm., **67**(12), 1183, (1988).

[49] S. Foner, B. Schwartz, Superconductor Materials Science, Plenum Press, NY, 1981.

[50] R.G. Hampshire, M.T. Taylor, J. Phys. **F2**, 89, (1972).

[51] H. Kumakura, H. Shimizu, K. Takahashi, K. Togano, H. Maeda, Jpn. J. Appl. Phys, **27**(4), L668, (1988).

[52] K. Togano, H. Kumakura, H. Maeda, E. Yanagisawa, K. Takahashi, Appl. Phys. Lett.,**53**(14), 1329 (1988).

[53] K. Setsune, K. Hirochi, H. Adachi, Y. Ichikawa, K. Wasa, Appl. Phys. Lett., **53**(7), 600, (1988).

[54] H. Iwasaki, N. Kobayashi, Y. Koike, M. Kikuchi, Y. Syono, K. Noto, Y. Muto, Jpn. J. Appl. Phys, **27**(9), L1631, (1988).

[55] Chemical Rubber Company Handbook of Physics, Edited by R.C. Weast, 52^{nd} Edition, 1971.

[56] T.T.M. Palstra, B. Batlogg, L.F. Schneemeyer, J.V. Waszczak, Phys. Rev. Lett., **61**(14), 1662, (1988).

[57] P.L. Gammel, L.F. Schneemeyer, J.V. Waszczak, D.J. Bishop, Phys. Rev. Lett., **61**(14), 1666, (1988).

[58] J.M. Tarascon, W.R. McKinnon, P. Barboux, D.M. Hwang, B.G. Bagley, L.H. Greene, G. Hull, Y. LePage, N. Stoffel, M. Giroud, Phys. Rev. **B38**(13), 8885 (1988).

[59] C.N.R. Rao, R. Vijayaraghavan, L. Ganapathi, S.V. Bhat, To be published in J. Solid State Chem., (1989).

[60] R. Ramesh, G. van Tendelco, G. Thomas, S. M. Green, H. L. Luo, Appl. Phys. Lett. **53**(22), 2220, (1988).

[61] R.M. Hazen, C.T. Prewitt, R.J. Angel, N.L. Ross, L.W. Finger, C.G. Hadidiacos, D.R. Veblen, P.J. Heaney, P.H. Hor, R.L. Meng, Y.Y. Sun, Y.Q. Wang, Y.Y. Xue, Z.J. Huang, L. Gao, J. Bechtold, C.W. Chu, Phys. Rev. Lett., **60**(12), 1174 (1988).

[62] N. Kijima, U. Endo, J. Tsuchiya, A. Sumiyama, M. Mizuno, Y. Oguri, Jpn. J. Appl. Phys. **27**(10), L1852, (1988).

[63] A. Ono, Jpn. J. Appl. Phys. **27**(7), L1213, (1988).

[64] K. Numata, K. Mori, H. Yamamoto, H. Sekine, K. Inoue, H. Maeda, J. Appl. Phys., **64**(11), 6392, (1988).

[65] U. Endo, S. Koyama, T. Kawi, Jpn. J. Appl. Phys. **27**(8), L1476, (1988).

[66] S.A. Sunshine, T. Siegrist. L.F. Schneemeyer, D.W. Murphy, R.J. Cava, B. Batlogg, R.B. van Dover, R.M. Fleming, S.H. Glarum, S. Nakahara, R. Farrow, J.J. Krajewski, S.M. Zahurak, J.V. Waszczak, J.H. Marshall, P.Marsh, L.W. Rupp, Jr., W.F. Peck, Phys. Rev. **B38**, 893, (1988).

[67] Liu Hongbao, Cao Liezhao, Zhou Ling, Mao Zhiqiang, Li Xiaoxian, Yu Zhidong, Xue Bai, Mao Xianglei, Zhou Guien, Run Yaozhong, Chen Zhaojia, Zhang Yuheng, Solid State Commun. **69**(8), 867, (1989).

[68] S. Geller, K.-Y. Wu, Appl. Phys. Lett., **54**(7), 669, (1989).

[69] T. Kawai, S. Kawai, S. Tanaka, T. Horiuchi, S.Takagi, K. Ogura, S. Kambe, M. Kawai, Jpn. J. Appl. Phys. **27**(12), L2296, (1988).

[70] S. Koyama, U. Endo, T. Kawai, Jpn. J. Appl. Phys., **27**(10), L1861, (1988).

[71] T. Hatano, K. Aota, S. Idea, K. Nakamura, K. Ogawa, Jpn. J. Appl. Phys. **27**(11), L2055, (1988).

[72] Y. Hakuraku, Y. Aridome, T. Ogushi, Jpn. J. Appl. Phys. **27**(11), L2091, (1988).

[73] D. Dimos, P. Chaudhari, J. Mannhart, F.K. LeGoues, Phys. Rev. Lett., **61**(2), 219, (1988).

[74] S.K. Dew, N.R. Osborne, B.T. Sullivan, P.J. Mulhern, R.R. Parsons, AIP Conf. Proc. **182**, AVS Series 6, (1989).

[75] M.J. Brett, J. Vac. Sci. Technol. **A6**(3), 1749, (1988).

[76] M.J. Brett, Journal of Materials Science, **24**, 623, (1989).

[77] D. Burbidge, P. Mulhern, S. Dew, R. Parsons, AIP Conf. Proc. **165**, AVS Series 3, 87, (1988).

[78] S.M. Rossnagel and J.J. Cuomo, AIP Conf. Proc. **165**, AVS Series 3, 106, (1988).

[79] H. Nobumasa, K. Shimizu, Y. Kitano, T. Kawai, Jpn. J. Appl. Phys. **27**(5), L846, (1988).

[80] A. Oota, A. Kirihigashi, Y. Sasaki, K. Ohba, Jpn. J. Appl. Phys. **27**(12), L2289, (1988).

[81] S.K. Dew, N.R. Osborne, P.J. Mulhern, R.R. Parsons, Appl. Phys. Lett., May 15, 1989.

[82] C.J. Kim, C.K. Rhee, H.G. Lee, C.T. Lee, S.J-L. Kang, D.Y. Won, Jpn. J. Appl. Phys. **28**(1), L45, (1989).

[83] S.K. Dew, N.R. Osborne, P.J. Mulhern, R.R. Parsons, to appear in Solid State Communications.

[84] N.R. Osborne, S.K. Dew, P.J. Mulhern, R.R. Parsons, submitted to ICMC 89 Conference Proceedings, (1989).

[85] M. Takano, J.Takada, K. Oda, H. Kitaguchi, Y. Miura, Y. Ikeda, Y. Tomii, H. Mazaki, Jpn. J. Appl. Phys. **27**(6), L1041, (1988).

[86] H. Nobumasa, T. Arima, K. Shimizu, Y. Otsuka, Y. Murata, T. Kawai, Jpn. J. Appl. Phys. **28**(1), L57, (1989).

[87] Y. Hakuraku, K. Kittaka, S. Higo, T. Ogushi, Jpn. J. Appl. Phys. **28**(1), L67, (1989).

[88] A. Ono, Jpn. J. Appl. Phys. **27**(12), L2276, (1988).

[89] T. Uzumaki, K. Yamanaka, N. Kamehara, K. Niwa, Jpn. J. Appl. Phys. **28**(1), L75, (1989).

[90] H. Nasu, T. Kato, S. Makida, T. Imura, Y. Osaka, Jpn. J. Appl. Phys. **27**(12), L2317, (1988).

[91] T. Yoshitake, T. Satoh, Y. Kubo, H. Igarashi, Jpn. J. Appl. Phys. **27**(7), L1262, (1988).

[92] K. Kuroda, M. Mukaida, S. Miyazawa, Jpn. J. Appl. Phys. **27**(11), L2230, (1988).

[93] M. Fukutomi, J. Machida, Y. Tanaka, T. Asano, T. Yamamoto, H. Maeda, Jpn. J. Appl. Phys. **27**(8), L1484, (1988).